LATE HOLOCENE PALEOCLIMATIC RECORDS FROM LAKE PAC CHEN AND CARWASH CENOTE, QUINTANA ROO, MEXICO

LATE HOLOCENE PALEOCLIMATIC RECORDS FROM LAKE PAC CHEN AND CARWASH CENOTE, QUINTANA ROO, MEXICO

ANYA KRYWY-JANZEN, B.Sc.

A Thesis

Submitted to the School of Graduate Studies

in Partial Fulfilment of the Requirements

for the Degree Master of Science

McMaster University

McMaster University
MASTER OF SCIENCE (2018)
Hamilton, Ontario, Canada
School of Geography and Earth Sciences

TITLE: **Late Holocene paleoclimatic records from Lake Pac Chen and Carwash Cenote, Quintana Roo, Mexico**

AUTHOR: Anya Krywy-Janzen, B.Sc. (McMaster University)

SUPERVISOR: Professor Eduard G. Reinhardt (McMaster University)

NUMBER OF PAGES: (xvii, 112)

ABSTRACT

The disintegration of the Classic Maya throughout the Terminal Classic (750-900 C.E.) is a complex loss of human population that has presented many questions about climate change and its impact on humanity. With droughts proposed as a prominent cause, understanding the quality and availability of groundwater resources at the time is pivotal to further determining the spatial and temporal distributions of population deterioration. The Yucatan aquifer consists of karstic cave systems, with a small number of inland lakes, which have previously been termed closed to the aquifer. It is important to understand how both of these types of water bodies react to long- and short-term forcing mechanisms such drying climate, sea-level rise and precipitation events. Using a variety of spatial and temporal records to determine aquifer evolution, changes and connectivity throughout the Holocene it will further understanding of how the aquifer reacts to changes in climate and the implications this may have had on the Classic Maya.

Four sediment cores from Pac Chen Lake and two sediment cores from Carwash Cenote were collected to investigate Holocene paleoclimatic trends on the Yucatan Peninsula in Mexico. Records of past climate, groundwater conditions and flooding history at both sites were determined through microfossil and micro X-Ray fluorescence data. In Pac Chen Lake, elevation and timing of flooding of the lake coincided with sea-level rise. Using Ti, Fe and K records to determine wet vs dry conditions, dry periods through the terminal classic coincided with other paleoclimate records, but with no evidence of draw-down within the lake. Both of these observations imply connection of the lake to the

aquifer. The Cl record from Carwash was used alongside a core from the Yax Chen cave system to observe spatial and temporal potability of the aquifer. An overall freshening trend in the coastal groundwater occurred throughout the Holocene. The largest amount of this freshening transpired through the Terminal Classic. At this time, populations inland were experiencing deterioration, while coastal populations along the coast continued to survive. Comparing Cl records at various depths and distances from the coast proved that Cl is impacted by proximity to the halocline.

ACKNOWLEDGEMENTS

As a someone who grew up with a great love for the earth and spending time outdoors, completing my MSc studying and exploring it has seemed like a dream. This accomplishment is very important to me and I have many people to thank for being alongside and supporting me through this process.

A huge thank you goes out to my supervisor, Dr. Eduard Reinhardt for not only providing the opportunity to work on such an amazing project, but also for fostering a love of scuba diving, being a great academic mentor and always taking us on adventures I never imagined I'd experience.

To my family, I wouldn't be here without you. Mom, you've always supported any endeavor I express interest in with all your heart. You've never believed any dream of mine to be too big, and your constant faith in my ability to achieve has always helped push me to do so.

Chelsi, I can't imagine having had anyone else by my side through this process. You are the best lab/field work partner, dive buddy and best friend I could've asked for. We've gone through many a wild ride together-I can't wait for all our future adventures and the day when we're cave diving together and freaking out about speleothems underwater.

To all my friends and colleagues within SGES over the years (Sian Ford, Aaron Coutino, Nick Riddick, Jeremy Gabriel, Mitchell Davidson and many more), you've all contributed to help make this an enjoyable process. Whether it be through beers at the

Phoenix, field work experiences or just listening to me rant, thank you for being so supporting and a group of people I'm happy to call my friends.

This project would not have been possible without the assistance from everyone I've worked with in Mexico. Fred Devos and Christopher le Maillot and the whole team at Zero Gravity for providing a home base as well as equipment and assistance during field work. All of the GUE cave divers that have graciously volunteered their time and talents over the years for the Mexico Cave Exploration Project (MCEP) and become friends and familiar faces I look forward to seeing every trip. Kelvin Davidson, I'm so happy to have had you as my Fundamentals instructor. Your sarcasm, life lessons and stories helped with the stress of trying to stay in place through valve drills.

Lastly, my field sites: Pac Chen and Carwash. Pac Chen stole two of our sensors and had terrible visibility to learn to core underwater for the first-time. Carwash gave me two miserable ear infections and helped me experience the Mexican healthcare system. Although I've gone through frustrations with both sites, without them this project would not have been possible.

DECLERATION OF ACADEMIC ACHIEVEMENT

Chapter 2- Water level rise recorded in Lake Pac Chen, Quintana Roo, Mexico infers connection with the aquifer and response to Holocene sea-

For this paper, all of the sediment cores were collected in the field by A. Krywy-Janzen, E. Reinhardt, P. van Hengstum and J. Gabriel. Lake column characteristics and water depth monitoring was completed by E. Reinhardt, S. Kovacs and A. Coutino. Laboratory samples were processed and analyzed by A. Krywy-Janzen and B. Waltham. Data analysis and figure creation was completed by A. Krywy-Janzen with aid/insight from E. Reinhardt. Manuscript has been prepared by A. Krywy-Janzen and E. Reinhardt.

Chapter 3- Long-term freshening of the coastal Yucatan aquifer since the mid-Holocene: Implications for groundwater potability through the Terminal Classic

For this paper, all of the sediment cores were collected in the field by A. Krywy-Janzen, C. McNeill-Jewer, P. van Hengstum and J. Gabriel. Cave survey was completed by 2017 MCEP volunteers: Hildegarden Wiggenhorn, Peter Gaertner, Sven Nellers and Mike Schernbeck. Hydrolab® CTD profile was collected by S. Kovacs. Laboratory samples were processed and analyzed by A. Krywy-Janzen. Data analysis and figure creation was completed by A. Krywy-Janzen with aid/insight from E. Reinhardt. Manuscript has been prepared by A. Krywy-Janzen and E. Reinhardt

TABLE OF CONTENTS

LIST OF FIGURES

CHAPTER 2

by a darker line. Red box represents timing of Maya Terminal Droughts based off both records and previous paleoclimate records. Bond events are represented by dashed red lines and cold/dry events by blue boxes. Cold/dry events are A) Little Ice Age 1300-1500 C.E., B) Dark Age/Migration Period Cooling 300-500 C.E. and C) Late Bronze Age Collapse 2.8-2.6 ka BP (Wanner et al., 2011).

Fig. 14 Salinity records from Carwash core 6 and Yax Chen core 4 and average temperature record from Greenland with major Maya archeological events. The Greenland temperature record comes from the GISP2 ice core from the summit region of central Greenland and temperature was reconstructed by using δ^{15}N and δ^{40}Ar gas fractionation within air bubbles in the ice to measure temperature gradients over time, which were then incorporated into a firn densification/heat diffusion model (Kiboshi et al., 2011). Records have been converted from Cl counts to ppt using equation created by McNeill-Jewer et al (in prep.). Yax Chen record is represented by red line and Carwash record is represented by green line, both records have a darker line that represents an ~50-100 yr running average. The Greenland temperature record is represented with a dark blue line, lighter blue band representing the 1σ error. Red box represents timing of Maya Terminal Droughts based off both records and previous paleoclimate records. Bond events are represented by dashed red lines and cold/dry events by blue boxes. Cold/dry events are A) Little Ice Age 1300-1500 C.E., B) Dark

Age/Migration Period Cooling 300-500 C.E. and C) Late Bronze Age Collapse 2.8-2.6 ka BP (Wanner et al., 2011).

LIST OF TABLES

CHAPTER 1

CHAPTER 2

CHAPTER 1-INTRODUCTION

The Yucatan Peninsula in Mexico is a large limestone carbonate that forms an area of approximately $165000\ \mathrm{km}^2$ (Ward et al., 1985). Glacioeaustacy, mixing-zone hydrology and litoral processes have significantly karstified the region, leading to numerous cave systems, dissolution lakes, aguadas and sinkholes, which allow for direct infiltration of precipitation to the aquifer and access to groundwater (Beddows, 2004; Smart et al., 2006). Cenotes are connected to the aquifer through conduits or cave passages, whereas aguadas are closed from the aquifer by a seal of organic or clay that has filled the sinkhole and lakes are draped in sediment (Flores-Nava, 1994). Paleoclimate studies that have termed their lakes as closed to the aquifer, typically refer to the sensitivity to climate change and δ^{18}O records that are mainly controlled by the evaporation-precipitation ratio (E/P), instead of groundwater inputs (Curtis et al., 1996; Hodell et al., 2005a). The Yucatan aquifer is that of a typical anchialine system; stratified by temperature and density. A lighter meteoric mass water mass overlies a warmer, denser marine mass, separated by the halocline, or mixing zone (Beddows, 2004; Smart et al., 2006; Beddows et al., 2007). The depth of this halocline increases inland at 1.6m/km alongside the thickness decreasing (Kovacs et al., 20189). These water masses have distinct differences, with the meteoric water mass having a salinity of 1-7ppt (decreasing inland) and average temperature of ~~25°C, and the marine having a salinity of 35ppt and average temperature of ~27°C (Stoessel, 1995; Stoessell and Coke, 2006; Kovacs et al., 2017a). As the aquifer is connected to the ocean through the karst, flooding of the coastal

cave systems was controlled by Holocene sea-level rise (Gabriel et al., 2009; Collins et al., 2015). However, evolution of sites further inland, such as lakes, that are typically thought to be closed off from the aquifer, has not been done in length. Monitoring of the coastal aquifer has revealed that changes in the meteoric water mass salinity is influenced by precipitation events and turbulent mixing, with larger events (in magnitude and time) eliciting a longer lasting and larger increase in salinity (Coutino et al., 2017; Kovacs et al., 2017b). Chan (2017) has looked at changes in salinity in the Yax Chen cave system throughout the Holocene, however further studies to spatially quantify response in the aquifer to climate changes are necessary.

The Classic Maya disintegration (750-1050 C.E.) is a comprehensively studied event as it embodies an extensive loss of population and culture. With multiple triggers proposed for the decline (warfare, storms, volcanic eruptions and deforestation), climate change continues to be the most prominent hypothesis (Brenner et al, 2002; McNeil et al, 2010; Kennett et al, 2012; Medina-Elizalde et al, 2016; Nooren et al, 2017). The spatial and temporal decline of the Maya has been proposed by Gill et al (2007) in three phases: the western lowlands at 810 C.E., the southeastern lowlands at 860 C.E. and lastly, the central and northern lowlands at 910 C.E. At the same time, populations in the north and along the coast were able to persist until the arrival of the Spanish (Dahlin, 2002; Masson, 2012). Many paleoclimate records have been collected throughout the Yucatan and using a wide range of proxies have found evidence of periods of drought through the Terminal Classic (Curtis et al., 1996; Haug et al., 2003; Hodell et al., 2005; Medina-Elizalde et al.,

2010; Kennett et al., 2012; Douglas et al., 2015). Using a wider range of proxies and spatial sites will help to further constrain this period of drought. Investigating the impact the climatic changes had on the aquifer and thus potable water resources is also important when considering spatial variability in the decline.

This dissertation is divided into two manuscripts for future publication. The first manuscript characterizes connectivity of the Yucatan aquifer further inland over time and how sea-level rise controls water level within the aquifer. The microfossil and μXRF records from four cores from Pac Chen Lake were used to recreate flooding history and environmental changes through the Terminal Classic. Used alongside water column characteristics and water depth monitoring, these records were then used to investigate connectivity of the lake to the aquifer over time. Using these records as well as previous paleoclimate studies, response in the lake on the shallow margin during the Classic Maya Droughts was investigated.

The second manuscript characterizes salinity changes within the coastal Yucatan aquifer through the Late Holocene. The microfossil and μXRF records from four cores from Carwash Cenote were used to recreate flooding history and hydrological changes within the meteoric water mass. The Cl record from Carwash was used alongside the Cl record from Yax Chen cave system to visualize these changes spatially and further determine how the aquifer is reacting to changes in climate and other variables. These changes were then compared to other Yucatan climate records and the timing of the Terminal Classic

droughts to determine the changes within the coastal aquifer at the time and how that may have impacted the Maya.

CHAPTER 2-Water level rise recorded in Lake Pac Chen Quintana Roo, Mexico infers connection with the aquifer and response to Holocene sea-level.

Authors: Anya Krywy-Janzen*[a], Eduard Reinhardt[a], Chelsi McNeill-Jewer[a], Aaron Coutino[b], Brenda Waltham[c], Marek Statsna[b], Dominique Rissolo[d], Sam Meacham[e], Peter van Hengstum[f]

[a] McMaster University, School of Geography and Earth Sciences, Hamilton, Ontario, L8S 4K1, Canada

[b] University of Waterloo, Department of Applied Mathematics, Waterloo, Ontario, N2L 3G1, Canada

[c] Department of Civil and Environmental Engineering, Carleton University, Ottawa Ontario

[d] Center of Interdisciplinary Science for Art, Architecture and Archeology at University of California-San Diego

[e] Mexico Cave Exploration Project (MCEP)

[f] Department of Marine Sciences, Texas A&M University-Galveston

[*] Corresponding author at: McMaster University, School of Geography and Earth Sciences, Hamilton Ontario, L8S 4K1, Canada. Email address: krywyja@mcmaster.ca

2.1 Abstract

The Maya civilization inhabited the Yucatan Peninsula in Mexico from over 3000 years ago until the decline of the Classic Maya between 750-900 C.E. A variety of mechanisms for its demise have been posed with droughts being a prominent cause. Four sediment cores taken in Pac Chen Lake (42km from the Atlantic Ocean and 22 km north of the Mayan village of Coba), Quintana Roo, Mexico, provide records of past climate and water level. PC1 Cores were taken at a depth of 25 m in the eastern basin (PC1) and three were taken along the southwestern margin over a depth interval of 0.5-6m (PC2-4). PC 1 documented flooding of the slopes at 800 B.C.E. and then flooding of the margins at 200 C.E. The basal ages of PC2 and PC4 coincide with this flooding of the margin. The elevation and timing of these flooding events match with reported sea-level rise for the Caribbean and indicates connection to the aquifer. The shallow margin cores documented reduced terrigenous input alongside the Classic Maya Droughts from other paleoclimate records, however no drawdown of water is occurring during this time. This also indicates connection to the aquifer as marine water intrusion from the coast would be replacing any evaporated freshwater.

2.2 Introduction

The decline of the Classic Maya civilization is seen as a significant loss of human culture and history and a potential analogue to modern demographic collapses (Costanza et al., 2007). A variety of different processes have been proposed that contributed to their

decline including warfare, climate change and storms, volcanic eruptions and deforestation (Brenner et al, 2001; McNeil et al, 2010; Kennett et al, 2012; Medina-Elizalde et al, 2016; Nooren et al, 2017). Droughts have been a prominent part of this discussion with a range of proxies being used from $\delta^{18}O$ records in speleothems and ostracods to sediment density (Hodell et al, 1995; Curtis et al, 1996; Hodell et al, 2005; Medina et al, 2010; Kennett et al, 2012). Previous studies have applied the inference that the lakes are closed, or effectively closed, to the aquifer and only responding to local environmental changes (Curtis et al., 1996; Brenner et al., 2002; Hodell et al., 2005). During periods of drought, the water level in these lakes is speculated to drastically change according to evapotranspiration regimes, but no quantitative volume changes have been stated or proven (Brenner et al., 2002; Hodell et al., 2005). Rise of water level in these lakes is concluded to mostly occur through increased rainfall, although some studies have considered rising sea level to potentially also contribute to this process (Brenner et al., 2002). For lake water level to be rising with sea level, there may be some sort of interconnectedness between the two that is more substantial than previously thought, however there is no data that has corroborated this possibility.

2.2.1 Paleoclimatic Records

The present climate of the Yucatan Peninsula is similar to other Caribbean regions, and the precipitation that occurs in the area is largely a result of the intertropical convergence zone (ITCZ) movements. The ITCZ is the equitorial low-pressure belt that comprises of the

convergence of the Northern and Southern Hemisphere trade winds (Hastenrath, 2013; Peterson et al, 1991). The north and southward movements of the ITCZ causes seasonal precipitation, with maximum levels occurring in early spring and late fall (Schneider et al., 2014). The dry season occurs December to April while the ITCZ is located farther south, which leads to a low seasonal precipitation of level of <100mm per month on average (Negreros-Castillo et al., 2003). Conversely, the wet season occurs May to November when the ITCZ has moved farther north and causes increased precipitation levels of 1000-1500 mm per month (Metcalfe et al., 2015). This precipitation is in turn lost by evapotranspiration (85%) and infiltration into the porous karst limestone (Smart et al, 2006; Beddows et al, 2007). Within the wet season, tropical storms and hurricanes are can make landfall on the peninsula causing high rainfall events, water level change, and aquifer hydrology changes (Kovacs et al., 2017a).

Previous paleoclimate records in the Yucatan Peninsula have occurred at many different sites, but some of the more cited and referenced research includes the sites of Lake Chichancanab, Punta Laguna, Chaac and Yok Balum stalagmites. All of these sites are located regionally within the Yucatan Peninsula, except Yok Balum Cave, which is located in Belize. The δ^{18}O records from Lake Punta Laguna by Curtis et al (1996) and Lake Chichancanab by Hodell et al. (1995) were generated by using various ostracods. The δ^{18}O records from Chaac and Yok Balum were compiled using microsamples of calcite along the stalagmite main growth axis (Medina et al, 2010; Kennett et al, 2012). Records from these locations revealed wet conditions from the Middle Preclassic to the Terminal Classic

Period (440-660 C.E.) and a drying trend during the Terminal Classic Period (660-1000 C.E.) followed by another period of drought (1020-1100 C.E.). Presence of gypsum precipitate in Lake Chichancanab indicated periods of decreased rainfall and/or increased evaporation over the Late Classic Period and Terminal Classic Period as water loss during these periods led to gypsum saturation within the lake. As the density signal varies greatly over this period, it was found that there was not a single large drought but interspersed periods of dry and wet climate with two drier phases (770-870 C.E. and 920-1100 C.E.) separated a period of wetter conditions (870-920 C.E.) (Hodell et al., 2005a). The consistencies seen between these five records support general interpretations made about the timing of wet and dry periods throughout the Holocene and an extended drought during the Terminal Classic Period. However, the role of climate change in the demise of the Classic Maya has been a very controversial subject because of uncertainties involved in dating climate and archeological records which has led to insufficient temporal resolution and variation between records (Hodell et al., 2005a).

2.2.2 Yucatan Hydrology

The Yucatan Peninsula in Mexico is an expansive limestone carbonate platform that separates the Gulf of Mexico and the Caribbean Sea. It is a tectonically stable, a low-lying platform that forms an area of approximately 165 000 km^2 (Ward et al., 1985). Mixing-zone hydrology, litoral process and glacioeustacy have created a heavily karstified countryside with extensive cave systems, dissolution lakes and sinkholes, allowing for

direct access to groundwater through aquifer resources (Beddows et al., 2004; Smart et al., 2006). In turn, most precipitation infiltrates through the porous limestone, which leads to no rivers and very few lakes (Perry et al., 2003). The aquifer system of the Yucatan Peninsula is temperature and density stratified like typical anchialine settings, with a meteoric water mass covering a mass of warmer intruding marine water (Beddows et al., 2007). These two masses are separated by the halocline, or mixing zone. Kovacs et al. (2017b) measured the current position of the halocline in Hoyo Negro to be approximately 18.5 m below current local water level, with depth increasing and thickness decreasing further inland from the coast (Beddows et al., 2004; Smart et al., 2006). There are very defined temperature and salinity differences between these two water masses, with the meteoric having a salinity of 1-7 ppt and an average temperature of ~ 25.0 °C, whereas the marine has a salinity of 35 ppt and average temperature of ~ 27.0 °C (Stoessell, 1995; Stoessell and Coke, 2006). The meteoric water mass has also been found to have higher salinities closer to the coast and decrease at a depth of 1.6 m/km (Kovacs et al., 2017a; Kovacs et al., 2018). Mixing of these two masses of water is not well understood, but has been observed to be affected through the movement of tides, drought and storm activity (Vera et al., 2012; Coutino et al., 2017; Kovacs et al., 2017). Beddows (2004) measured the hydraulic gradient of the aquifer in the Yucatan to be $5.79*10^{-5} \pm 3.00*10^{-7}$, which causes groundwater level to rise inland relative to sea level by approximately 10 - 15 cm/km.

Within the peninsula, water bodies are sinkhole lakes that are either classified as cenotes or aguadas formed by the collapse or dissolution of the karstic limestone (Hodell et al.,

2005b). Cenotes are connected to the aquifer through conduits or cave passages, whereas aguadas are closed from the aquifer by a seal of organic or clay that has filled the sinkhole (Flores-Nava, 1994). Paleoclimate studies that have termed their lakes as closed to the aquifer, typically refer to the sensitivity to climate change and δ^{18}O records that are mainly controlled by the evaporation-precipitation ratio (E/P), instead of groundwater inputs (Curtis et al., 1996; Hodell et al., 2005a). An organic/clay basin seal has also been linked to reasoning as to why some of these lakes are closed, but there can still be significant water loss through downward leakage when the lake has a seal (Deevey, 1988; Hodell et al., 2005b) Sinkhole lakes can change between open and closed to the aquifer throughout their lifetimes, depending on sediment accumulation on the bottom (Hodell et al., 2005b). Connection to the aquifer can lead to connection to the ocean and is shown to be dependent on how connected to the ocean the conduit is as well as its distance from the coast (Beddows, 2004; Valle-Levinson et al., 2011; Null et al., 2014).

2.2.3 Pac Chen Lake

Pac Chen Lake is an enclosed freshwater system consisting of three individual basins with an area of approximately 36735m^2, located in the Quintana Roo province of Mexico (Fig. 1). It lies approximately 42 km from the Atlantic Ocean and roughly 22 km north of the Maya village of Coba. The shores are surrounded by vegetation with a village and Eco Tour Centre sit on the west side of the lake. The bottom of Pac Chen is draped with sediment and there are no known conduits that are connecting it to the aquifer, making it easy to

assume that it can be considered an aguada. However, there is a cenote and cave system to the southeast of Pac Chen, indicating that there are conduits within the vicinity. There are no significant archaeological sites in the area but Coba a large Lat Classic period Mayan city (550-850 C.E.) is ~ 20 km due south from the lake (Leyden et al., 1998).

2.2.4 XRF Core Scanning

The method of analyzing cores for bulk elements through XRF is noninvasive and is explained in greater detail in Micro-XRF Studies of Sediment Cores (Croudace and Guy Rothwell, 2015). Increases in titanium, iron and potassium in bulk sediment are used to indicate input of terrigenous material and therefore increased precipitation levels (Haug et al., 2003; Pierce 2012). The titanium record from Cariaco Basin (off Northern Venezuela) was used to interpret regional hydrological changes and the changes in the position of the ITCZ over time as Ti increases in the record were correlated with dark laminae depositions that were rich in terrigenous grains (Haug et al., 2003). The Cariaco Basin and Maya lowlands are both located in the northern limits of the ITCZ, so while it is southward during the dry season, there is a lower input of Ti in the basin sediment. During the Terminal Classic Collapse, a similar decrease of Ti input was seen, indicating decrease in precipitation. A sediment core taken in Lake Chalco, a high altitude closed lacustrine basin within the Basin of Mexico, was analyzed for iron and potassium using a Cox Itrax uXRF core scanner (Pierce 2012). Spikes in in Fe and K matched with tephra and

terrigenous layers within the core, and decreases in both of these along with Ca were used to show a shift towards more arid conditions.

2.2.5 Testate Amoebae (Arcellaceans)

Testate amoebae are single-celled protists with a secreted or agglutinated test that are found in freshwater to brackish environments and are sensitive to pH changes, trophic state and salinity (Charman, 2001; Patterson and Kumar, 2002; Van Hengstum et al., 2008). Testate amoebae have previously been used to determine climate changes, paleohydrology, sea-level reconstruction and limnological variables (Reinhardt et al., 1998; Scott et al., 2001; Patterson and Kumar, 2002; Gabriel et al., 2009, Van Hengstum et al., 2010)**.** Many studies of testate amoeba in lakes look at surface sediment to determine distribution of species (Dalby et al., 2000; Roe and Patterson, 2006; Escobar et al., 2008; Van Hengstum et al., 2008). Different testate amoebae found include species of the following genera: *Arcella, Centropyxis*, *Cyclopyxis*, *Difflugia, Cucurbitella, Lesquereusia, Euglypha*, *Trinema*, *Corythion, Polysaccammina, Miliammina,* and *Jadaminna.* In assemblages within tropical regions, testate amoebae usually occur in low abundances and low species diversities and are dominated by centropyxids (Dalby et al., 2000; Roe and Patterson, 2006). Testate amoebae have been used alongside foraminifera to determine the zonation between them in salt marshes, or other environments with oligohaline conditions (0.5 - 5 psu) (Gehrels et al., 2001; Riveiros et al., 2007). As testate amoebae are sensitive to parameters other than salinity, identifying salinity as the

foremost control to taxonomic gradation in these environments with large daily fluctuations in conditions is difficult. Other complications with these studies can include the presence of soil testate amoeba taxa in lower salt marsh assemblages and larger faunal changes in taxonomic subtleties than what are wanted occur (Gehrels et al., 2001). This indicates that the testate amoebae in salt marshes are tending to document the larger changes in salinity only. In cenotes in the Yucatan Peninsula, testate amoebae were used alongside foraminifera to document salinity changes and how it affected the assemblages (Van Hengstum et al., 2008). A shift from testate amoebae-dominated assemblages to foraminifera-dominated was found at ~ 3.5 psu, along with testate amoebae morphotypes without spines (*Centropyxis aculeata* "discoides") being more prominent over those with (*Centropyxis aculeata* "aculeata") as salinity increased. This change in morphotype and decrease in abundance in samples could be seen between fairly small changes in salinity (1.5 to 2.9 psu and 3.4 to 3.7 psu).

2.3 Methods

2.3.1 Sediment Cores

i) Core Locations

Four sediment cores were recovered in Pac Chen using self-contained underwater breathing apparatus (SCUBA). PC1 was collected in the eastern basin at a depth of 25 m, and was 182 cm long. PC2, 3 and 4 were collected in a transect along the southwestern margin at depths of 5 m, 3 m and 0.5 m and are 66cm, 86cm and 98cm long respectively

(Fig. 2 and 3). These cores were taken on the margin right below a slope to best record terrigenous input.

ii) Sediment Analyses

The bulk sediment trace element composition of the cores was analyzed using a Cox Analytical Systems Itrax uXRF core scanner. PC 2, 3 and 4 were left intact, and therefore the undisturbed core was analyzed using the Chromium heavy element (Cr-HE) X-ray source (30kv, 10mA, exp. time = 15s, step-size = 500µm). As PC 1 was collected previously and subsampled into bags at 1cm intervals, the Sequential Sample Reservoir (SSR) vessel was used with the same parameters as above, and measurements from within each reservoir were averaged (Gregory et al, 2017).

For microfossils, PC1, 2 and 4 were analyzed. The 1.25cm^3 samples were disaggregated and then wet sieved through a 45µm screen to concentrate microfossils. Samples were subdivided into 8 aliquots using a wet splitter outlined in Scott and Hermelin (1993) to achieve raw counts of at least 100 individuals where possible. Microfossils were wet counted using an Olympus SZX12 table microscope (max. 135X) and identified based on published taxonomic data (Medioli and Scott, 1983; Scott et al., 2001). Data is represented as fractional abundances (F_i) in % of total counted specimens and was calculated using

$$F_i = \frac{C_i}{N_i}$$

where C_i is the number of individuals of a species and N_i is the total number of individuals in the sample. As so few species and individuals were present, all species were determined to be significant and used for analyses.

iii) Radiocarbon Dating

Twelve radiocarbon samples were obtained from the four cores. Samples consisted of twigs, charcoal or bulk organic matter (OM) and were pretreated with acid/alkali/acid wash and sent to Direct AMS for analysis. The R statistical software package Clam 2.2 (Blaauw, 2010; version 2.2) was used with the northern hemisphere calibration curve IntCal13 (Reimer et al., 2013) to calibrate the raw radiocarbon ages presented as ranges in calibrated years before present (cal BP) to a 2σ confidence interval. A linear age model was used to fit the data, and sedimentation accumulations were calculated, along with interpolated ages throughout cores. Calibrated years BP (yr BP) are used unless otherwise noted.

2.3.2 Pac Chen Lake Characteristics

Water depth in Pac Chen was measured using a ReefNet Sensus Ultra water depth sensor, which is normally used for diving but has also been used for logging long-term water depths in groundwater (Kovacs et al., 2017a). The sensor was securely attached to piling of the dock located on the west side of the lake near the Alltournative tourist facility at ~ 2.9 m depth. The sensor resolves depth to 1.27 cm with an accuracy of ± 30.48 cm and to 0.1 °C with an accuracy of ± 0.8 °C. Depth measurements were recorded every 30 minutes

over May 12-21, 2016.For comparison with the aquifer a depth sensor was also placed in Yax Chen Cenote covering May 1-10, 2016. As the sensors only measure pressure, typically a hydrostatic approximation is made about the water column. To solve this equation a surface boundary condition is required which is the atmospheric pressure data, which was recorded by a HOBO Water Level Data Logger placed in the mangroves near Yax Chen Cenote which is part of the Ox Bel Ha cave system (Collins et al., 2015, Coutino et al., 2017, Kovacs et al. 2017). While it would be possible to assume the typical atmospheric pressure, by using a separate pressure sensor in the atmosphere we can get a much more accurate calculation for the water depth. However, since the atmospheric pressure sensor measurement times are not aligned to the water pressure sensor the data was interpolated in MATLAB. A cubic spline interpolation was used. Once the data was aligned the hydrostatic equation was solved to give water depth.

A depth conductivity, temperature profile was measured for Pac Chen using a YSI Model 30 conductivity meter. The probe was lowered through the water column at 1 m increments up to a depth of 15.5 m. The probe was calibrated with salinity standard solutions (brackish) before measurements. The instrument resolves specific conductivity to 1.0 µS/cm with an accuracy of ± 0.5% FS and resolves temperature to 0.1 °C with an accuracy of ± 0.1°C. A depth profile of the lake was created by taking a transect on the surface, from the west to east shores, using the Archer Field PC GPS receiver and a Vexilar LPS-1 Digital Handheld Depth Sounder which was calibrated and verified with a weighted tape measure at several points along the transect.

2.4 RESULTS

2.4.1 Core Lithology

PC1, which was from the deep basin (-25 m), contains dark, fine-grained OM (organic matter; 120 - 185 cm) with increasing carbonate content (marl and shells) towards the top of the core (0 - 120 cm). Intact and fragmented gastropods are found throughout the core as well as wood and leaf fragments (Fig. 6). PC2 which was collected at -5 m depth is composed of marl and fine OM with distinct beds of higher or lower OM content (eg. 50 and 29 cm; Fig 7). Intact and fragmented gastropods are also present, but to a lesser extent than the other cores. PC3 and PC4 which were collected at - 3 and -0.5 m water depth also contain marl and fine OM, but also have a bed of coarser OM and gastropod shells from ~ 52 - 63 cm in PC 3 and ~ 40 - 50 cm in PC 4 (Fig. 8, 9). PC4 also has OM rich units at ~ 9 - 12, 16 - 22 and 91 - 95 cm.

2.4.2 Age Models

Radiocarbon ages show no reversals with a maximum basal age of 2904 - 2974 B.C.E. in PC1 and 138 - 281 C.E. in PC4 (Fig. 11; Table 1). The age models for PC1 to 4 are generally linear with some changes in accumulation rates. PC 1 has relatively high accumulation rates between ~ 37 - 181 cm (0.037 - 0.2927 cm/yr) with lower accumulation rates from ~ 0 - 37 cm (0.0144 - 0.0343 cm/yr). The average rate over the entire length of the core (181 cm) is 0.097 cm/yr. In PC 4, the accumulation rate from 0 - 77 cm was linear at ~ 0.04

cm/yr but the rate was higher from 77 - 94 cm (0.4 cm/yr). The average accumulation rate in PC4 (0.14 cm/yr) was ~ 1.5 X higher than PC1.

2.4.3 Water Body Characteristics

Surface water in Pac Chen has a measured salinity of 0.5 ppt with a thermocline at ~ 5 m where there is a ~ 3 º C drop in temperature and specific conductivity (SEC; ~ 40 mS/cm; Fig. 4).

The water depth measured from May 12 to 21 2017 shows tidal water level changes in Pac Chen (Fig. 5). A time-propagating semi-diurnal tidal variation is evident with regular periodicity, showing an ~ 3 - 4 cm change in water depth with amplitudes of ~ 12 - 13 hours which matches the M_2 tidal constituent of 12.42 hours (Talley et al., 2011; Fig. 5). Spring and neap tides are also likely contributing to larger amplitude changes at 0.5 month periodicity is evident as well. Tidal measurements at Puerto Morelos show a similar semi-diurnal tidal periodicity with an ~ 10 - 20 cm range (Para et al., 2015). Pac Chen is a small lake (~ 300 m x 125 m) with low fetch, so waves will only have a minor effect on water depth changes.

The diurnal water depth changes (~ 10 - 12 cm) associated with tidal frequency were also found in our a nearby groundwater level monitoring station in Yax Chen cenote which have also examined previously and also shown here (Fig. 5; Coutino et al., 2017; Kovacs et al. 2017b; Kovacs et al., 2018).

2.4.4 µXRF Core Records

The PC1 records for Ti, Fe, K show similar trends spanning the last ~ 4 ka. Values are relatively high from ~ 2000 B.C.E. to ~ 400 B.C.E. and then quickly decline until ~ 200 C.E. after which they remain relatively constant albeit with a slight reduction until present. Calcium shows an inverse trend increasing over the past ~ 4 ka which matches changes in sediment color, with lighter colours representing higher carbonate (shells and marl) vs OM content. The Inc/Coh values which can be a measure of OM content and porosity of the sediment are inversely correlated with Ca but show only minor trends with Fe, Ti and K (Jouve et al., 2013**;** Fig. 6 and 10).

Cores from the shallow margin of Pac Chen (PC2, 3, 4) show similarly in their Ti, Fe, K records, but they are lower in magnitude relative to PC1 and the overall variation in values is not as great (Fig. 7, 8 and 9). Ti, Fe and K all co-vary in the cores, except K in PC3, which does differ compared to Ti and Fe. Ca and Inc/Coh also show similar relationships as described for PC1, but do not vary to the same extent, since the sediment is a gradation of marls and OM compared to PC1, which has intervals with higher OM content. There are two gastropod concentrations in PC3 (56 - 63 cm) and PC4 (40 - 50 cm), but otherwise are largely undifferentiated marls and OM. PC4 has an OM unit at the base and has higher OM contents at the top of the core relative to PC3, but otherwise all the shallow margin cores have similar lithologies.

2.4.5 Microfaunal Assemblages

In PC 1, *Centropyxis aculeata, Centropyxis constricta* were the dominant taxa with *Difflugia oblonga* present only in minor abundance ($\lesssim$ 5%) along with two additional unidentified taxa which were also minor (Fig. 6). These minor taxa were only found in the upper 40 cm of the core. In PC2 and 4, the dominant taxa was *C. aculeata* with minor abundance of *C. constricta* and there was no clear trend in the cores (Fig. 7 and 9).

2.5 Discussion

2.5.1 Longterm Lake Level and Sea Level Rise

Based on the evidence in the sediment cores, there is a progression of flooding that appears to match Holocene sea level rise and thus has important implications for connectivity of the lake to the aquifer. Evidence for this flooding sequence is from the change in sediment rate and composition found in the deep basin core PC1 and the basal age of the shallow margin core PC4 (Fig. 13). If the lake is connected to the aquifer as we surmise, and the aquifer is in turn responding to sea level rise as has been demonstrated in previous studies, the bottom of the lake would have been flooded by at least ~ 10 -11 ka. Our basal age for PC1 is ~ 4 ka (~ 2000 B.C.E), so water level was already at ~ -2 to -3 m below present at this stage, but may have been closer to -5 m. The near basal age of PC2 which was collected at ~ -5 m is ~ 2.5 ka indicating that water level was at this point at least by this time, but perhaps earlier, because we don't have an age for the bottom of the core, and this elevation may have been flooded but not accreting sediment prior to

this date. This lack of sediment accumulation with water level rise has been noted in previous studies which examined groundwater elevation and Holocene sea-level rise in cave sediments (Collins et al., 2015). The sill separating the two deep basins was connected by ~ 2.5 ka but the areal extent of the lake was slightly smaller than present. Holocene sea level had already begun it's deceleration at ~ 6 - 7 ka, but the slowed water level rise after 2.5 ka allowed wetlands to develop (Fig. 14; Khan et al., 2017). These fringing wetlands began baffling and accreting sediments on the shallow sloped margin reducing sediment input to the deep basin. This change in the loci of sedimentation is evidenced by the higher amount of terrigenous elements (Ti, Fe and K) in the basal portion of PC1 relative to the top, and the decrease in sediment accumulation at ~ 1.8 ka (PC4). This timing for the change in sedimentation in PC1 corresponds to the age for the flooding and accretion of sediments on the shallow lake margin (PC4) which occurred at ~ 1.8 ka and matches the timing and elevation of Holocene sea levels rise. However, the change in sediment composition (Ti, Fe and K) in PC1 also coincides within increased carbonate content of the sediment (Ca) and decreased Inc/Coh values, so the decrease in Ti, Fe and K is also a matrix effect with uXRF analysis. However, the increased carbonate content in PC1 is originating from this newly created biogenic production in the shallow wetland environment with the rising water level after 2.5 ka, and thus still records changing sediment sources with water level rise. A similar trend was found in Little Spring in Florida, where flooding of the shallow sloped margin caused wetland development and increased OM deposition in the deep basin (Gregory et al., 2017). Also, sediment accumulation in

PC2, which is at -5 m depth stops at ~ 1.9 ka which is close to the timing for the onset of sedimentation in PC4 at ~ 1.8 ka, also indicating this preferential trapping of sediment in the lake margin wetlands.

2.5.2 Open, Leaky or Closed?

This progression of flooding and its effect on sedimentation over the past ~ 4 ka in Pac Chen suggests that the lake is connected to the aquifer and responding to sea level rise. Presently, the water level in Pac Chen shows a diurnal tidal pattern, which has been found in long-term monitoring of groundwater level in nearby cave systems (Coutino et al., 2017; Kovacs et al., 2017b). This indicates that the basin is connected to the aquifer but is hydrologically isolated (i.e. leaky) as proposed by other studies (Curtis et al., 1996; Hodell et al., 2005a). It is unclear how much interchange occurs, but there seems to be a significant residence time since there is a distinct thermocline at - 6 m and the bottom water temperature is ~ 24 º C while groundwater temperatures are ~ 25 - 26 ºC (Kovacs et al, 2018; Coutino et al., 2017; Beddows 2004). These groundwater temperatures are closer to the coast, but the 1 ºC cooler temperature suggests that there is limited interchange with groundwater. Rainfall generally is cooler, which has been observed in reduced aquifer temperatures after rainfall events, so it is likely the lake water is largely derived from rainfall (Coutino et al., 2017; Kovacs et al., 2018). So presently, water level is responding to tidal fluctuations, but is a separate water body (hydrologically isolated) that is affected by seasonal changes in evaporation and precipitation. Over the long term,

sea-level appears to be controlling lake water level, but it is unknown the degree of interchange with the aquifer as surrounding karst is flooded, but especially before sediment begins to blanket its margins occluding the highly porous limestone. Therefore caution should be used when interpreting long term paleoclimatic records in these lakes, but especially those that are recording changing lake chemistry as they are maybe affected by changing aquifer condition.

2.5.3 Lake Water Drawdown During Classic Mayan Droughts

Previous lake studies examining paleoclimatic records of the classic Mayan droughts have referred to lake level drawdown during the droughts which is predicated on the lakes being closed or leaky basins (Curtis et al., 1996; Brenner et al., 2002; Hodell et al., 2005b). However, there have been no studies examining lake margin stratigraphic sequences to test this hypothesis. Based on our previous discussion regarding lake connectivity to the aquifer with sea-level rise, there would be no significant water level drop during droughts. Groundwater level, and thus Pac Chen lake level, will be largely controlled by sea-level because of the anchialine hydrology and the highly porous nature of the Yucatan karst (Fig. 16; Collins et al., 2015). During dry periods, the meteoric water mass would be thinner, but seawater would intrude from the coast replacing this missing freshwater, resulting in little net change of water level (Kovacs et al., 2017a). Based on our core transect, this seems to be the case, as there is no evidence in PC2 - 4 showing lake level change during the Classic Mayan droughts (Fig. 12). PC4 which is the shallowest

core (- 0.25 m) shows OM at the base, which likely represents a shallow wetland as the karst is initially flooded, followed by an interval of carbonate mud indicative of deeper water and then an increase in OM towards the top of the core as sedimentation infills the reducing accommodation space causing shallowing. The only notable interval within this sequence of sediments is the gastropod shell layer (~ 40 - 50 cm) which dates to the Mayan droughts (~ 750 - 1100 C.E.; 1250 - 900 yrs BP), but doesn't appear to be related to water depth (Hodell et al., 2005a) Gastropods don't dominate the upper portion of PC4 which is at - 0.5 m and observations of the modern surface found no existing concentrations. PC3 is more carbonate mud rich, suggestive of deeper conditions as the core was collected at - 3 m and further away from the fringing wetland vegetation. Again, the only notable feature is another gastropod layer (~ 56 - 63 cm) with slightly higher OM contents, which has a younger age to that in PC4 (~ 750 vs 1100 yrs BP), but does not date to the period of droughts (900 - 1250 yrs BP). The gastropod layer in PC4 could be interpreted as a slight decrease in water depth during the time of the droughts (< 0.5 m), which may be the case, but there is no evidence of subaerial exposure. There is no depositional hiatuses or roots indicating a water level drop, nor are there indurated or cemented layers which can occur with subaerial exposure in carbonate mud rich sediments. However, the concentration of gastropods may relate to changing salinity or other ecological effects of the droughts, but the gastropod layers don't appear to be reliable indicator of changing water depth. Based on this evidence, at least in Pac Chen, the water level during the droughts does not seem

to have been significantly lower and the lake would have largely remained at its current size in terms of areal extent.

2.5.4 Fidelity of uXRF Core Records

The elemental records from PC1 are not sufficient to resolve the effects of the Mayan droughts on the lake, because of the reduced sediment accumulation in the deep basin (< 2.5 ka) and also because of the lower sample resolution (cm). PC1 also has relationships between Fe, Ti, K, Ca and Inc/Coh values indicating that the record is more affected by matrix effects with the uXRF analysis as has already been discussed (Fig. 10). PC2 - 4 have more consistent lithologies, and we focus on PC4 as it records the effect of the drought, with a good sediment accumulation rate and age resolution. PC4's location is also closest to the source of weathering inputs from the surrounding karst terrain and thus better records climate changes vs the deeper cores.

Fe, Ti and K show direct interrelationships and have collectively been used as terrigenous weathering proxies in marine and lake basins as well as coastal lagoons (Gregory et al., 2015). During wet periods there is more chemical weathering and input of weathering product into basins with the increased precipitation, and conversely during dry periods there is less (Haug et al., 2003; Chague - Goff et al., 2016). The Ti record in PC4 is not as useful as Fe and K, because Ti concentration is not high enough within some portions of the core. Fe and K however, are within the detection limits of the uXRF and co-vary with only minor differences. Because the Yucatan peninsula is composed of

limestone, there is little clastic sediment for a source of Fe, so most of the Fe oxyhydroxides deposited in the lake basin originate from dissolution of limestone and aeolian dust sources (Norris & Rohl, 1999). K also has a similar source, but can also be secondarily concentrated in plant material, but would be expected to behave similarly during wet periods with increased OM decay and input to the lake basin with increased runoff from the land surface (Steinke et al., 1993).

There is an indirect relationship between K and Inc/Coh in PC2 - 4, but also a large spread in values, and Fe shows little relationship with Inc/Coh. However, Fe and K both still share similar trend in the cores. K will be more affected by changes in OM content in the sediment because of the secondary plant source, while Fe will be less so, because its source is largely from lithogenic weathering of limestone and aeolian dust. So there is an overall minor matrix affect with K which is in part OM dependant, but the K trend towards lower values towards the top of PC4 seems to be a primary environmental signal as it is replicated in the Fe record. Fe, may be affected by redox diagenesis, while Ti and K will be unaffected by post depositional migration within the sediment, although this doesn't appear to be significant as Fe covaries similarly with K and Ti (Kylander et al., 2011).

2.5.5 Potassium Record of the Classic Mayan Droughts

The K record from PC4 spanning the last 1.6 ka shows an overall decreasing trend, and based on the previous discussion, a trend towards drier conditions with an inflexion point at ~ 0.7 ka (1300 C.E.). Proxy records from other nearby locations on the Yucatan

do not show this overall trend, neither the Chaac speleothem, nor the Punta Laguna or Lake Chichancanab records, although the Punta Laguna record does show highly variable and low $d^{18}O$ values from ~ 950 yrs BP to present (Fig. 15; Curtis et al., 1996; Hodell et al., 2005a; Medina-Elizalde et al., 2010). The Yok Balum speleothem from Belize has the best correspondence with our K record from Pac Chen, showing an overall drying trend, but also an inflection point at 0.7 ka (Kennet et al., 2012). It doesn't appear that this overall K trend is significantly affected by matrix effects associated with uXRF analysis as discussed previously.

During the Mayan droughts, there is also a rapid drop in K values from ~ 960 - 1160 yrs BP (840 - 1040 C.E.) that spans the Terminal Classic to Early Postclassic transition (~ 950 C.E.). The decrease in K is between ~ 45 - 55 cm in PC4, which does overlap the gastropod layer between ~ 40 - 50 cm, so there may be a slight matrix affect with these values (Fig. 9). However, the reduction in K between 45-50 cm which is in the marly sediment below the gastropod layer indicates that the drop in values is a primary signal, vs a matrix effect (Fig. 9). This drop in K values matches the droughts recorded in Punta Laguna at ~ 940 - 1160 yrs BP (840 - 1160 C.E.) and Lake Chichancanab at ~ 940 - 1250 yrs BP (750 - 1060 C.E.) which record changing water chemistry ($d^{18}O$ and gypsum/sediment density g/cm^3; Curtis et al., 1996; Hodell et al., 2005a). These proxies may be more responsive to short term variations vs weathering and eventual input of K and Fe through runoff into the lake basin, although the density record in Lake Chichancanab is a binary record, responding once the evaporative threshold for gypsum precipitation has been

reached, and thus would only record extreme dry periods. The nearby Punta Laguna $d^{18}O$ would be more sensitive over a wider range of evaporative change than the gypsum, but both of these records show two drought phases while our Pac Chen K record only shows one, albeit with short term fluctuations during this time period (Fig. 15; Curtis et al., 1996; Hodell et al., 2005a). The speleothem $d^{18}O$ records which will be sensitive and high resolution, show some similarity as well, with droughts coinciding with the Pac Chen dry period as defined by our K record (Medina-Elizalde et al., 2010; Kennett et al., 2012).

Overall, K and Fe show good correspondence with the previously established drought records, but are perhaps not as sensitive for recording temporal changes. Slight differences in age for the drought period can be attributed to inaccuracies in radiometric dating of the various proxies (i.e. sediment and speleothem) and their individual sensitivities in recording environmental change (Hodell et al., 2015a) . However, uXRF core scanning of shallow lake sediments does show potential, even if it may not be as sensitive as other proxies, but it can provide additional information on weathering inputs of terrigenous sediment into the lake basin which may provide additional insight on the droughts, but also anthropogenic effects of Mayan forest clearing and agriculture in other settings (Torrescano-Valle and Islebe, 2015; Battistel et al., 2018).

2.6 Conclusions

This study documenting the deep basin to the shallow margin stratigraphy of Pac Chen Lake shows that water level is largely controlled by rising Holocene sea-level and

thus the lake is connected to the aquifer. Water column characteristics (temperature, conductivity) and water depth monitoring (tidal influence) reinforces this interpretation, but also suggests that the lake is hydrologically closed or leaky, thus recording climatic changes. This condition however, may have changed through the flooding progression. This connection with the aquifer, coupled with a lack of stratigraphic evidence, indicates that there was little, to no lake drawdown during the Classic Maya droughts, because marine water intrusion from the coast would replace the reduced amount of freshwater thus keeping water level at its original position.

The shallow margin cores also show reduced terrigenous weathering inputs (K, Fe) with the Classic Maya Droughts that match other paleoclimatic records from nearby lakes and speleothem. These weathering proxy indicators (K, Fe) are hindered by lags in their production and input to the lake so thus do not record short term changes in rainfall that have been documented with other proxies. However, they can be useful especially when considering the resolution and efficiencies of uXRF core scanning, and these high-resolution records may show utility for examining Mayan impacts due to land clearance and agriculture.

2.7 Acknowledgements

The authors would like to thank Zero Gravity Dive shop and the Mexican Cave Exploration Project for dive support and logistics. Special thanks to Fabián Arriaga for allowing us access to Pac Chen and for permission to take sediment cores and place sensors. Funding

was provided by National Sciences and Engingeering Research Council of Canada (EGR-Discovery).

2.8 References

Battistel D., Roman M., Marchetti A., Kehrwald N., Radaelli M., Balliana E., Toscano G. and Barbante C. (2018). Anthropogenic impact in the Maya Lowlands of Petén, Guatemala, during the last 5500 years. *Journal of Quaternary Science* **33** 166-176.

Beddows, P. A. (2004). Groundwater hydrology of a coastal conduit carbonate aquifer: Caribbean coast of the Yucatán Peninsula, México (Doctoral dissertation, University of Bristol).

Beddows P., Smart P., Whitaker F., Smith S. (2007) Decoupled fresh-saline groundwater circulation of a coastal carbonate aquifer: Spatial patterns of temperature and specific electrical conductivity. *Journal of Hydrology* **346**, 18-32.

Blaauw, M. (2010) Methods and code for "classical" age-modelling of radiocarbon sequences. *Quaternary Geochronology* **5**, 512-518.

Brenner M., Hodell D., Curtis J., Rosenmeier M., Binford M. and Abbott M. (2001). Abrupt climate change and pre-Columbian cultural collapse. *Interhemispheric Climate Linkages*, 87-103.

Brenner M., Rosenmeier M., Hodell D. and Curtis J. (2002). PALEOLIMNOLOGY OF THE MAYA LOWLANDS: Long-term perspectives on interactions among climate, environment, and humans. *Ancient Mesoamerica* **13**, 141-157.

Charmon D. (2001) Biostratigraphic and palaeoenvironmental applications for testate amoebae. *Quaternary Science Reviews* **20**, 1753-1764.

Chague-Goff C., Chan J., Goff J. and Gadd P. (2016) Late Holocene record of environmental changes, cyclones and tsunamis in a coastal lake, Mangaia, Cook Islands. *Island Arc* **25**, 333-349.

Collins S., Reinhardt E., Rissolo D., Chatters J., Nava Blank A. and Luna Erreguerena P. (2015) Reconstructing water level in Hoyo Negro, Quintana Roo, Mexico, implications for early Paleoamerican and faunal access. *Quaternary Science Reviews* **124**, 68-83.

Coutino A., Statsna M., Kovacs S. and Reinhardt E. (2017) Hurricanes Ingrid and Manuel (2013) and their impact on the salinity of the Meteoric Water Mass, Quintana Roo, Mexico. *Journal of Hydrology* **551**, 715-729.

Croudace I. and Guy Rothwell R. (2015) Micro-XRF studies of sediments cores: applications of a non-destructive tool for the environmental sciences (developments in paleoenvironmental research). *Tracking Environmental Change Using Lake Sediments. Volume 2: Physical and Geochemical Methods* **2**, 464.

Curtis J., Hodell D. and Brenner M. (1996) Climate variability on the Yucatan Peninsula (Mexico) during the past 3500 years, and implications for Maya cultural evolution. *Journal of Quaterary Research* **46**, 37-47.

Deevey, E. S. (1988). Estimation of downward leakage from Florida lakes. *Limnology and Oceanography* **33**, 1308-1320.

Flores-Nava, A. (1994). Some limnological data from five water bodies of Yucatan as a basis for agriculture development. *Anales del Instituto de Ciencias del Mar y Limnologia* **1-2**, 1-153.

Gabriel J., Reinhardt E., Peros M., Davidson D., van Hengstum P., and Beddows P. (2008) Paleoenvironmental evolution of Cenote Aktun Ha (Carwash) on the Yucatan Peninsula, Mexico and its response to Holocene sea-level rise. *Journal of Paleolimnology* **42**, 199-213.

Gehrels W., Roe H. and Charman D. (2001) Foraminifera, testate amoebae and diatoms as sea-level indicators in UK saltmarshes: A quantitative multiproxy approach. *Journal of Quaternary Science* **3**, 201-220.

Gregory B., Peros M., Reinhardt E. and Donnelly J. (2015) Middle-late Holocene Caribbean aridity inferred from foraminifera and elemental data in sediment cores from two Cuban lagoons. *Palaeogeography, Palaeoclimatology, Palaeoecology* **426**, 229-241.

Gregory B., Reinhardt E. and Glifford J. (2017) The influence of morphology on sinkhole sedimentation at Little Salt Spring, Florida. *Journal of Coastal Research* **33**, 359-371.

Hastenrath S. and Polzin D. (2013) Climatic variations in Central America and the Caribbean. *International Journal of Climatology* **33**, 1348-1356.

Haug G., Gunther D., Peterson L., Sigman D., Hughen K. and Aeschlimann B. (2003) Climate and the collapse of Maya civilization. *Science* **299**, 1731-1735.

Hodell D., Curtis J. and Brenner M. (1995) Possible role of climate in the collapse of Classic Maya civilization. *Nature* **375**, 391-394.

Hodell D., Brenner M., Curtis J. and Guilderson T. (2001) Solar Forcing of Drought Frequency in the Maya Lowlands. *Science* **292**, 1367-1370.

Hodell D., Brenner M., Curtis J. (2005) Terminal Classic drought in the northern Maya lowlands inferred from multiple sediment cores in Lake Chichancanab (Mexico). *Quaternary Science Reviews* **24**, 1413-1427.

Hodell D., Brenner M., Curtis J., Medina-Gonzales R., Ildefonso-Chan Can E., Albornaz-Pat A. and Guilderson T. (2005) Climate change on the Yucatan Peninsula during the Little Ice Age. *Quaternary Research* **63**, 109-121.

Jouve G., Francus P., Lamoureux S., Provencher-Nolet L., Hanh A., Habberzettl T., Fortin D., Nuttin L. and The PASADO Science Team (2013). Microsedimentological characterization using image analysis and m-XRF as indicators of sedimentary processes and climate changes during Lateglacial at

Laguna Potrok Aike, Santa Cruz, Argentina. *Quaternary Science Reviews* **71**, 191-204.

Kennett D., Brietenbach S., Aquino V., Asmerom Y., Awe J., Baldini J., Bartlein P., Culleton B., Ebert C., Jazwa C., Macri M., Marwan N., Polyak V., Prufer K., Ridlel H., Sodemann H., Winterhalder B. and Haug G. (2012) Development and disintegration of Maya political systems in response to climate change. *Science* **338**, 788-791.

Khan N., Ashe E., Horton B., Dutton A., Kopp R., Brocard G., Englehart S., Hill D., Peltier W., Vane C. and Scatena F. (2017) Drivers of Holocene sea-level change in the Caribbean. *Quaternary Science Reviews* **155**, 13-36.

Kovacs S., Reinhardt E., Chatters J., Rissolo D., Schwarcz H., Collins S., Kim S.T., Nava Blank A. and Luna Erreguerena P. (2017) Calcite raft geochemistry as a hydrological proxy for Holocene aquifer conditions in Hoyo Negro and Ich Balam (Sac Actun Cave System), Quintana Roo, Mexico. *Quaternary Science Reviews* **10**, 205-214.

Kovacs S., Reinhardt E., Statsna M., Coutino A., Werner C., Collins S., Devos F., Le Maillot C. (2017) Hurricane Ingrid and Tropical Storm Hanna's effects on the salinity of the coastal aquifer, Quintana Roo, Mexico. *Journal of Hydrology* **551**, 704-714.

Kovacs S., Reinhardt E., Werner C., Kim S.T., Devos F., and Le Maillot C. (2018) Seasonal trends in calcite-raft precipitation from cenotes Rainbow, Feno and Monkey Dust, Quintana Roo, Mexico: Implications for paleoenvironmental studies. *Palaeogeography, Palaeoclimatology, Palaeoecology* **497**, 157-167.

Kylander M., Ampel L, Wohlfarth B. and Veres D. (2011). High-resolution X-ray fluorescence core scanning analysis of Les Echets (France) sedimentary sequence: new insights from chemical proxies. *Journal of Quaternary Science* **26**, 109-117.

Leyden B., Brenner M. and Dahlin B. (1998) Cultural and climatic history of Coba, a Lowland Maya City in Quintana Roo, Mexico. *Quaternary Research* **49**, 111-122.

Lind C. (1971) Specific conductance as a means of estimating ionic strength. *U.S. Geological Survey Professional Paper* **P 0700-D**, D272-D280.

McNeil C., Burney D. and Burney L. (2010). Evidence disputing deforestation as the cause for the collapse of the ancient Maya polity of Copan, Honduras. *Proceedings of the National Academy of Sciences* **107**, 1017-1022.

Medina-Elizalde M., Burns S., Lea D., ASmerom Y., von Gunten L., Polyak V., Vuille M., and Karmalkar A. (2010) High resolution stalagmite climate record from the Yucatan Peninsula spanning the Maya terminal classic period. *Earth and Planetary Science Letters* **298**, 255-262.

Medioli F. and Scott D. (1986) Lacustrine thecamoebians (mainly arcelleans) as potential tools for palaeolimnological interpretations. *Palaeo* **62**, 361-386.

Metcalfe S.E., Street-Perrott F.A., O'Hara S.L., Hales P.E., and Perrot R.A. (1994) The paleolimnological record of environmental change: Examples from arid frontier of Mesoamerica. *Environmental change in drylands; biogeographical and geomorphological perspectives*, 131-145.

Metcalfe S., Barron J., and Davies S. (2015) The Holocene history of the North American Monsoon: 'known knowns' and 'known unknowns' in understanding its spatial and temporal complexity. *Quaternary Science Review* **120**, 1-27..

Negreros-Castillo P., Snook L. and Mize C. (2003) Regenerating mahogany (Sweietenia macrophyllia) from seed in Quintana Roo, Mexico: The effects of sowing method and clearing treatment. *Forest Ecology and Management* **183**, 351-362.

Nooren K., Hoek W., van der Plicht H., Sigl M., van Bergen M., Galop D., Torrescano-Valle N., Islebe G., Huizinga A., Winkes T. and Middelkoop H. (2017).

Explosive eruption of El Chichon volcano (Mexico) disrupted 6th century Maya civilization and contributed to global cooling. *Geology* **45**, 175-178.

Norris R. D., and Röhl U. (1999). Carbon cycling and chronology of climate warming during the Palaeocene/Eocene transition. *Nature* **401**, 775.

Null, K. A., Knee, K. L., Crook, E. D., de Sieyes, N. R., Rebolledo-Vieyra, M., Hernández-Terrones, L., & Paytan, A. (2014). Composition and fluxes of submarine groundwater along the Caribbean coast of the Yucatan Peninsula. *Continental Shelf Research* 77, 38-50.

Patterson T. and Fishbein E. (1989) Re-examination of the statistical methods used to determine the number of point counts needed for micropaleontological quantitative research. *Journal of Paleontology* **63**, 245-248.

Patterson T. and Kumar A. (2002) A review of current testate rhizopod (thecamoebian) research in Canada. *Palaeo* **180**, 225-251.

Perry E., Paytan A., Pedersen B. and Velazquez-Oliman G. (2009) Groundwater geochemistry of the Yucatan Peninsula, Mexico; constraints on stratigraphy and hydrogeology. *Journal of Hydrology* **367**, 27-40.

Perry E., Velazquez Oliman G. and Wagner, N. (2011) Preliminary investigation of groundwater and surface water geochemistry in Campeche and Southern quintana roo. In: Spring, Ú.O. (Ed.), Water Resources in Mexico. Springer, Berlin, 87-97.

Peterson, L., Overpeck J., Kipp N., and Imbrie J. (1991), A high-resolution late Quaternary upwelling record from the anoxic Cariaco basin, Venezuela, *Paleoceanography* **6**, 99–119.

Pierce M. (2012) A 40,000 year geochemical record from Lake Chalco, Mexico (Master's Thesis). Retrieved from: http://www.d.umn.edu/dees/research/thesis/Rubesch_Megan_April2012.pdf

Reimer P. J., Bard M.G.L., Bayliss A., Beck J.W., Blackwell P.G., Ramsey C.B., Buck C.E., Edwards R.L., Freidrich M., Groots P.M., Guilderson T.P., Haflidason H., Hajdas I., Hatté C., Heaton T.J., Hoffmann D.L., Hogg A.G., Hughen K.A., Kaiser K.F., Kromer B., Manning S.W., Nui M., Reimer R.W., Richards D.A., Scott E.M., Southon J.R., Turney C.S.M., and van der Plicht J. (2013), IntCal13 and Marine13 radiocarbon age calibration curves, 0-50,000 years Cal BP. *Radiocarbon* **55**, 1896-1887. Schmitter-Soto.

Reinhardt E., Dalby A., Kuma, A., & Patterson, R. T. (1998). Arcellaceans as pollution indicators in mine tailing contaminated lakes near Cobalt, Ontario, Canada. *Micropaleontology*, 131-148.

Riveiro, N., Babalola A., Boudreau R., Patterson R.T., Roe H. and Doherty C. (2007). Modern distribution of salt marsh foraminifera and thecamoebians in the Seymour–Belize Inlet Complex, British Columbia, Canada. *Marine Geology* **242**, 39-63.

Scott D.B. and Hermelin J.O.R. (1993) A device for precision splitting of micropaleontological samples in liquid suspension. *Journal of Paleontology* **67**, 151-154.

Scott D., Medioli F., and Schafer C. (2001) Monitering in coastal environments using foraminifera and thecamoebians. *Cambridge University Press, New York, USA.*

Smart P.L, Beddows P.A., Doerr S., Smith S.L. and Whitaker F.F. (2006) Cave development on the Caribbean coast of the Yucatan Peninsula, Quintana Roo, Mexico. *Geological Society of America Special Paper 404: Perspectives on Kart Geomorphology, Hydrology, & Geochemistry,* 105-128, doi:10.1130/2006. 2404(10).

Steinke, T. D., Holland, A. J., & Singh, Y. (1993). Leaching losses during decomposition of mangrove leaf litter. *South African Journal of Botany* **59**, 21-25.

Stoessel R. (1995) Dampening of transverse dispersion in the halocline in karst limestone in the northeastern Yucatan Peninsula. *Groundwater* **33**, 366-371.

Stoessel R. and Coke J. (2006) An explanation for the lack of dilute freshwater lens in unconfined tropical aquifers: Yucatan example. *Gulf Coast Association of Geological Societies Transactions* **56**, 785-792.

Talley L., Pickard G., Emery W. and Swift J. (2011) Gravity Waves, Tides, and Coastal Oceonography. *Descriptive physical oceanography: an introduction*, 223-244. Academic press.

Torrescano-Valle N. and Islebe G. (2015) Holocene paleoecology, climate history and human influence in the southwestern Yucatan Peninsula. *Review of Palaeobotany and Palynology* **217**, 1-8.

Valle-Levinson A., Marino-Tapia I., Enriquez C., and Waterhouse A. F. (2011). Tidal variability of salinity and velocity fields related to intense point-source submarine groundwater discharges into the coastal ocean. Limnology and Oceanography **56**, 1213-1224.

van Hengstum P., Reinhardt E., Beddows P., Huang R. and Gabriel J. (2008) Thecamoebians (Testate Amoebae) and foraminifera from three anchialine cenotes in Mexico: low salinity (1.5-4.5 psu) faunal transitions. *Journal of Foraminiferal Research* **38**, 305-317.

van Hengstum P., Reinhardt E., Beddows P., and Gabriel J. (2010) Linkages between Holocene paleoclimate and paleohydrology preserved in a Yucatan underwater cave. *Quaternary Science Reviews* **29**, 2788-2798.

Vera, I., Mariño-Tapia, I., & Enriquez, C. (2012). Effects of drought and subtidal sea-level variability on salt intrusion in a coastal karst aquifer. *Marine and Freshwater Research* **63**, 485-493.

Ward W., Weidi A. and Back W. (1985) Geology and hydrogeology of the Yucatan and Quaternary geology of Northeastern Yucatan Peninsula. *New Orleans Geological Society*, 1-160.

2.9 Figures

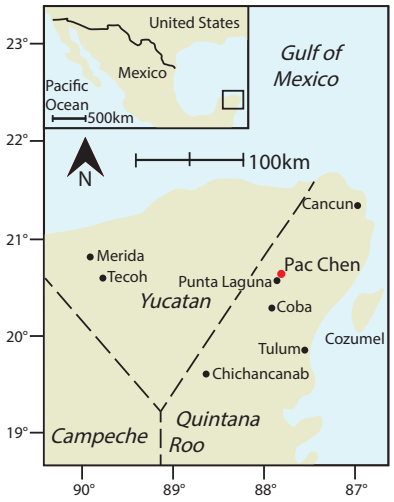

Fig. 1-Map of study area in Yucatan Peninsula, Mexico. Location of Pac Chen Lake denoted by red circle. Black circles denote location of modern cities and paleoclimate record sites.

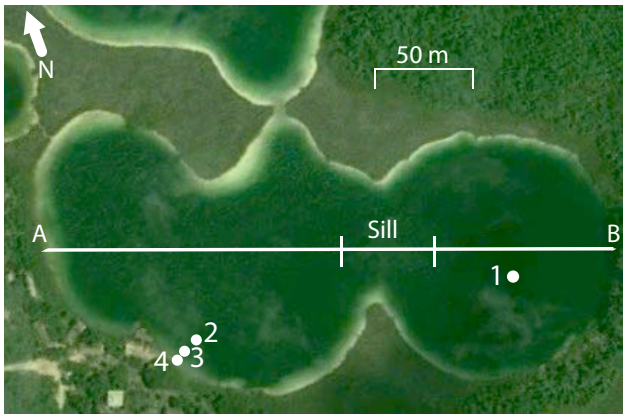

Fig.2- Google Earth image of Pac Chen Lake. White line denotes lake transect for the depth profile (Fig. 3) and white circles denote core locations.

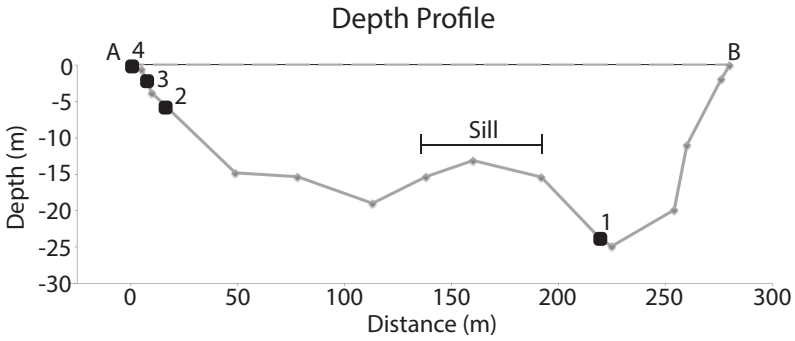

Fig. 3- Depth profile of Pac Chen Lake with core depths denoted by black circles

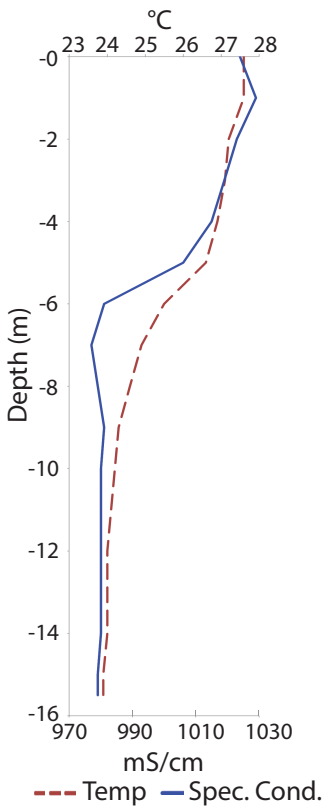

Fig. 4- Temperature and specific conductivity depth profile of Pac Chen Lake. Temperature is represented by dashed red line. Specific conductivity is represented by blue solid line.

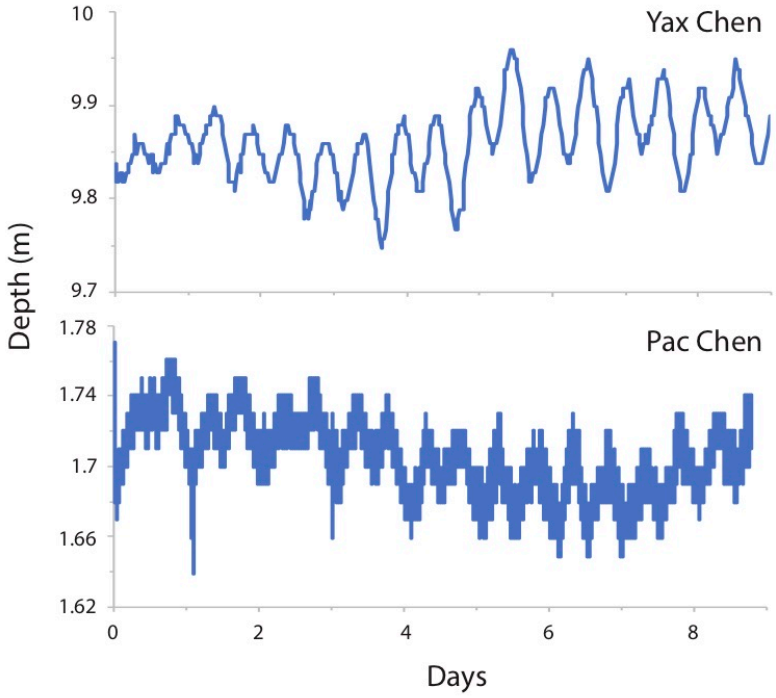

Fig. 5- Nine days of water level data from Yax Chen Cenote which is part of the Ox Bel Ha Cave System and Pac Chen Lake. Yax Chen data covers May 1-10, 2016. Pac Chen data covers May 12-21, 2016.

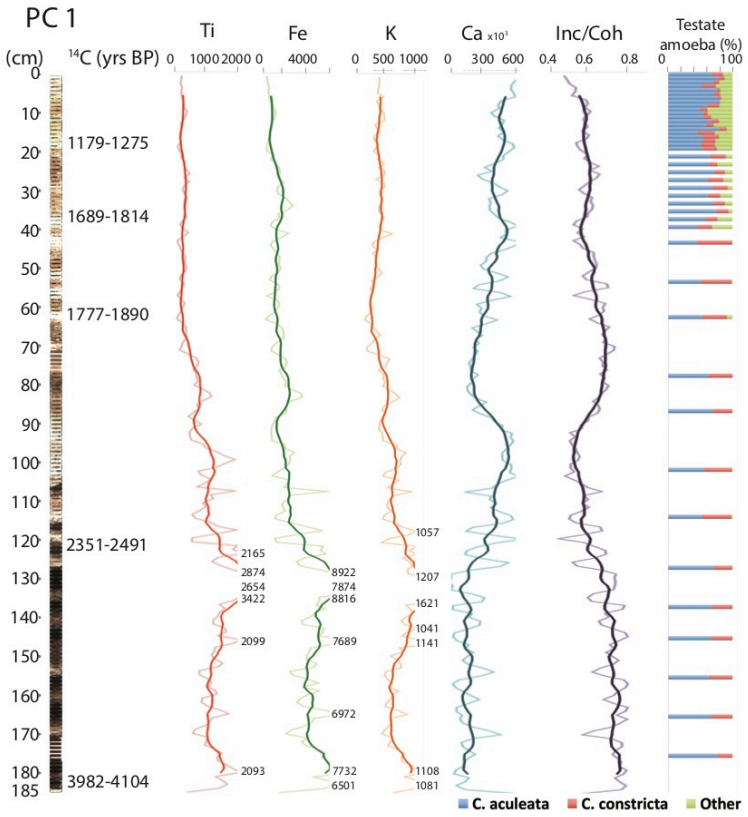

Fig. 6- Pac Chen Core 1 (PC1) with radiocarbon dates, µXRF (Ti, Fe, K, Ca and Inc/Coh) and microfossil data (*C. aculeata, C. constricta* and other). Radiocarbon dates are in calibrated yrs BP, µXRF data in mean total counts per cm, and microfossil data in % of total counts.

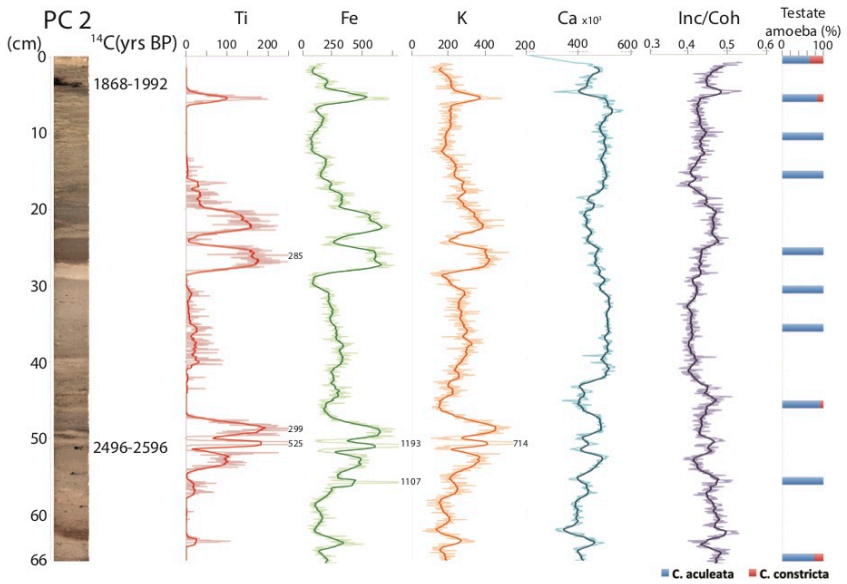

Fig. 7- Pac Chen Core 2 (PC2) with radiocarbon dates, µXRF (Ti, Fe, K, Ca, and Inc/Coh) and microfossil data (*C. aculeata* and *C. constricta*). Radiocarbon dates are in calibrated yrs BP, µXRF data in total counts per 500 µm, and microfossil data in % of total counts.

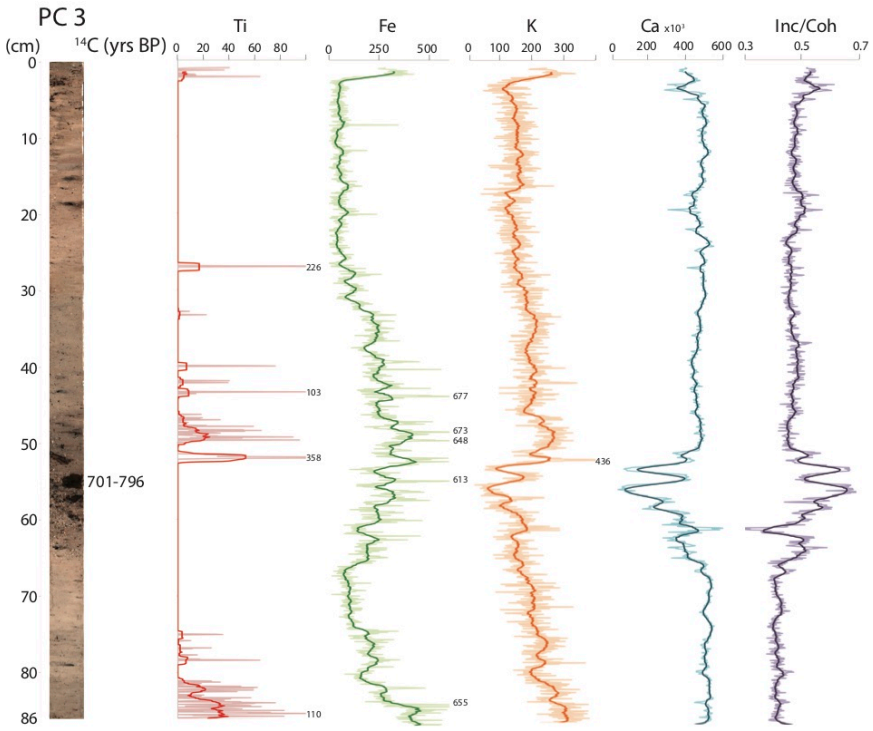

Fig. 8- Pac Chen Core 3 (PC3) with radiocarbon dates and µXRF (Ti, Fe K, Ca, and Inc/Coh) data. Radiocarbon dates are in calibrated yrs BP and µXRF data in total counts per 500 µm.

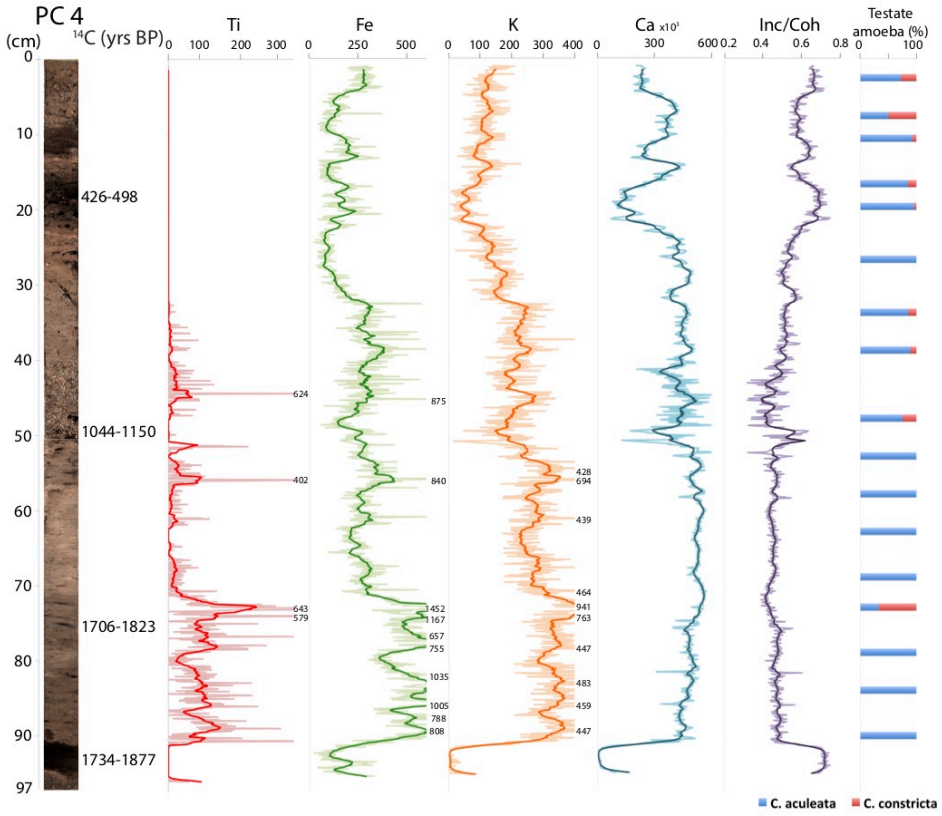

Fig. 9- Pac Chen Core 4 (PC4) with radiocarbon dates, µXRF (Ti, Fe, K, Ca, and Inc/Coh) and microfossil data (*C. aculeata* and *C. constricta*). Radiocarbon dates are in calibrated yrs BP, µXRF data in total counts per 500 µm, and microfossil data in % of total counts.

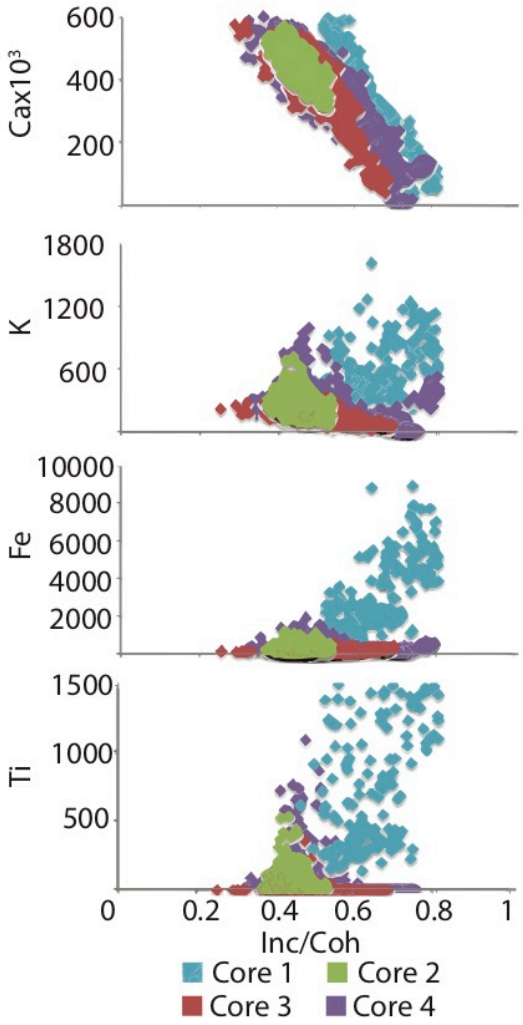

Fig. 10- Cross-plots of total Inc/Coh versus total Ti, Fe, K and Ca counts from all cores.

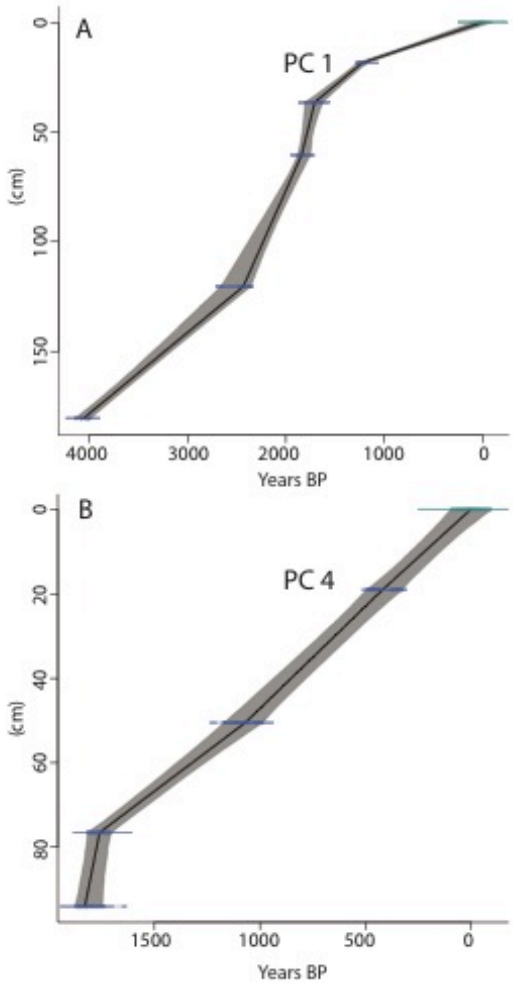

Fig. 11- Age models constructed for PC1 and 4 using Clam 2.1 (R; Blaauw, 2010; Reimer et al., 2013). Blue lines represent calibrated distribution of dated material through the length of the cores. Grey area represents calibrated age ranges (yrs. BP) at 2σ confidence intervals.

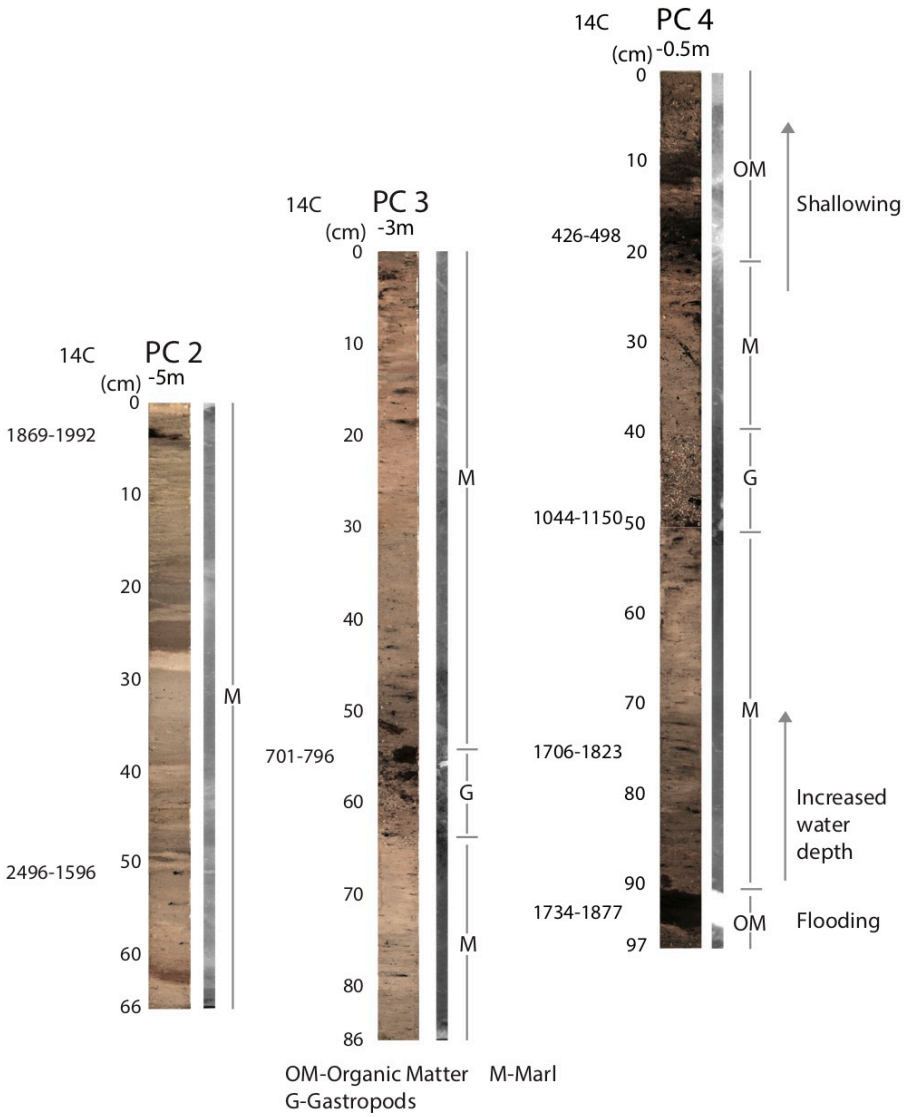

Fig. 12- Images of cores PC2, 3 and 4 with calibrated radiocarbon dates in yrs BP, water depths and lithological composition.

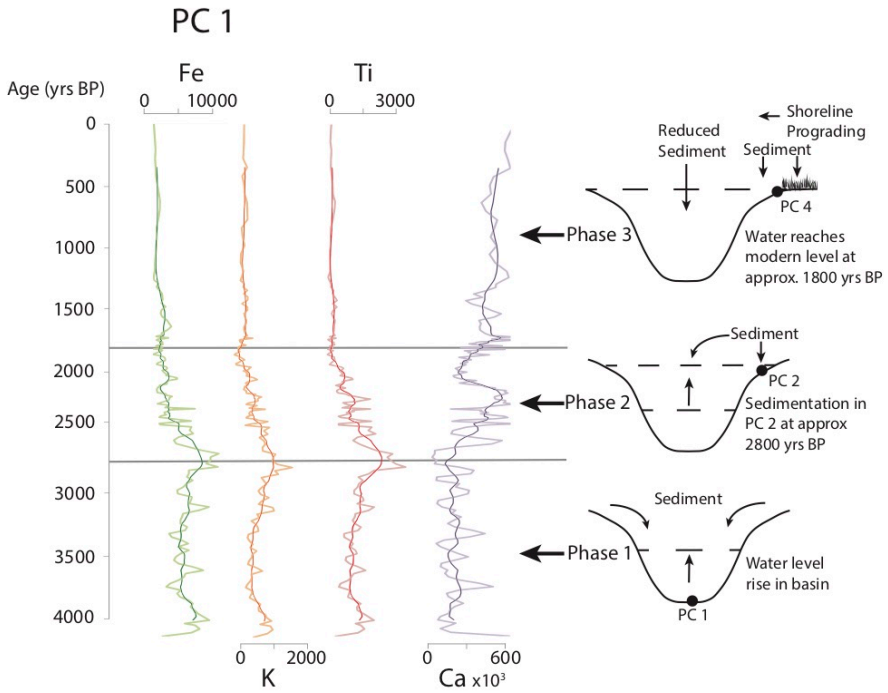

Fig. 13- Evolution of Pac Chen Lake with associated changes in Fe, K, Ti and Ca in PC 1. Three phases of flooding evolution are depicted.

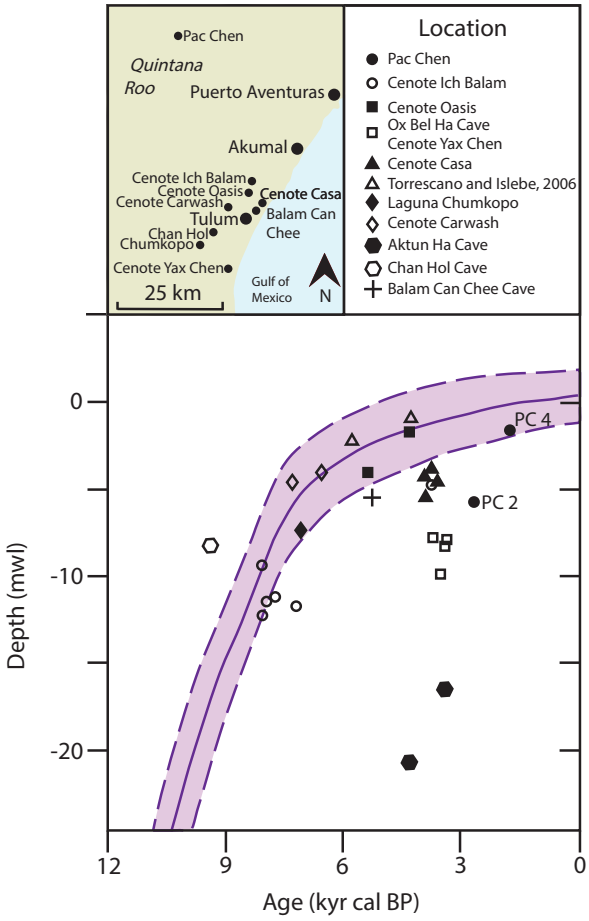

Fig. 14- Mexico sea-level curve from Khan et al (2017) where middle purple line denotes the mean and shaded purple area within two dashed purple line denotes 2σ confidence interval. Radiocarbon age of basal (PC4) and near basal elevation of PC2 with flooding dates for the aquifer from Cenotes Ich Balam, Oasis, Yax Chen Cave system, Casa Cenote, El Palmar Swamp, Laguna Chumkopó, Cenote Carwash and associated cave system Aktun Ha (Collins et al. 2015a, Torrescano and Islebe 2006, Brown et al. 2014, Gabriel et al. 2009, van Hengstum et al. 2010).

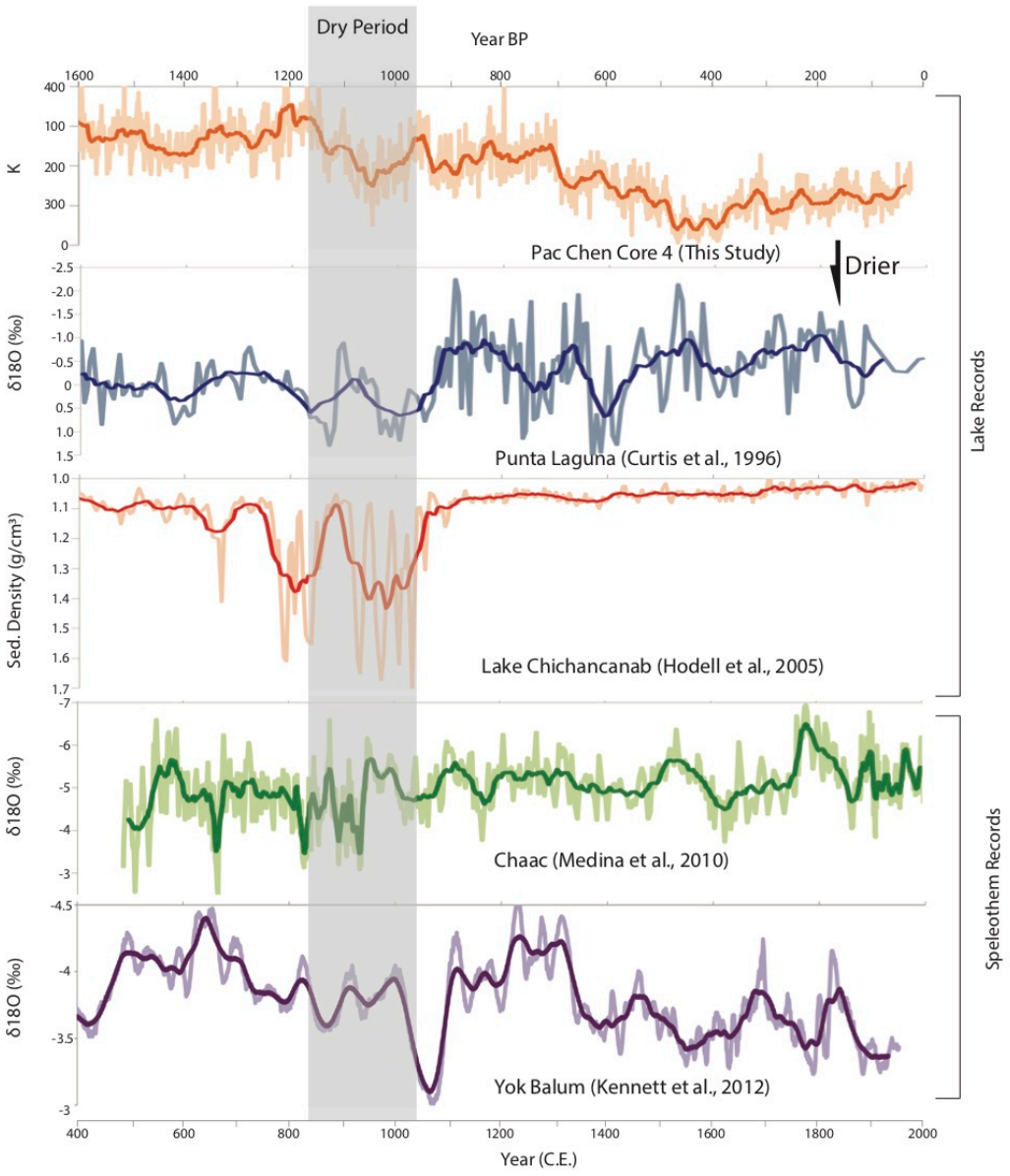

Fig 15- Comparison of PC4 potassium record with paleoclimate records from Punta Laguna (δ18O; Curtis et al., 1996), Lake Chichancanab (sediment density; Hodell et al., 2005), Chaac speleothem (δ18O; Medina et al., 2010), and Yok Balum speleothem (δ18O; Kennet et al., 2012). The grey box denotes the dry period defined by the Pac Chen potassium record.

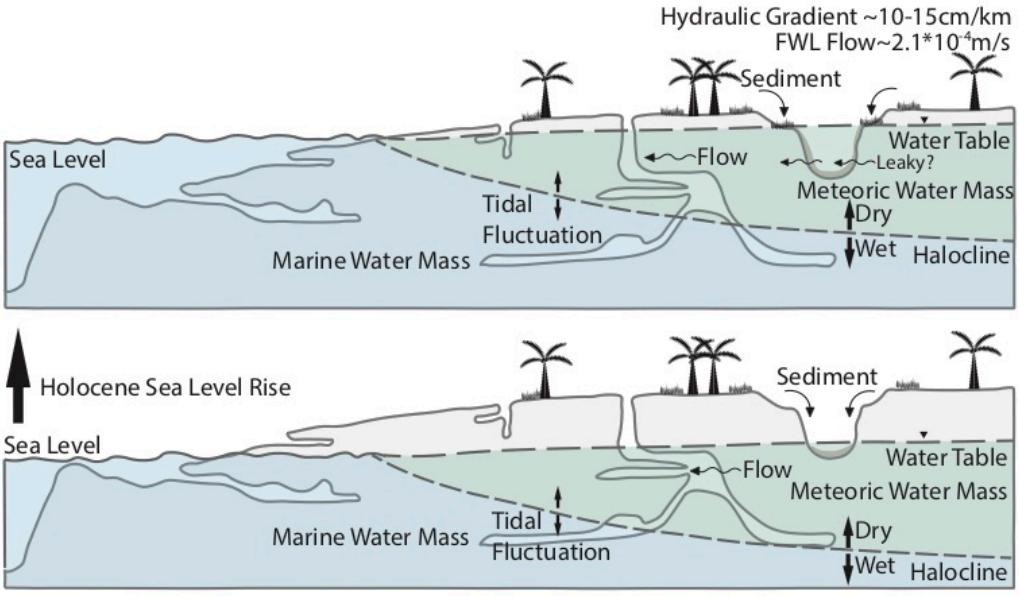

Fig. 16- Diagrammatic evolution of Yucatan aquifer with Holocene sea-level rise. Marine and Meteoric water masses are depicted as well as movement of the halocline with tidal fluctuations and relative wet vs dry climates. Holocene sea-level causes rising groundwater within the highly porous karst to flood cave systems and cenotes and depressions within the karst (aquadas and lakes). Sedimentation at the bottom and sides of the depressions, can then affect interchange between the lake and aquifer water resulting in hydrologically isolated basins, but may still respond to sea-level change.

2.10 Tables

Table 1- Radiocarbon results from Pac Chen Lake.

Core	Lab ID D-AMS	(cm)	Material	^{14}C Age (±2σ yr BP)	Cal yr BP (2σ)	C.E./B.C.E.
1	008976	18.5	OM	1273±24	1179-1275	732-828
	008977	36.5	OM	1788±27	1689-1814	193-318
	008362	60.5	OM	1891±23	1777-1890	117-230
	008363	120.5	OM	2403±27	2351-2491	484-344
	008365	180.5	OM	3717±27	3982-4104	2091-1974
2	013073	3.5	OM	1970±30	1868-1992	23-147
	013074	51.5	Twig	2535±29	2496-2596	581-481
3	013078	54.5	Twig	857±23	701-796	1219-1314
4	013071	19	Twig	367±24	426-498	1517-1589
	013072	50.5	Twig	1153±24	1044-1150	865-971
	013077	76.5	Charcoal	1825±24	1706-1823	192-309
	013070	94	Twig	1876±26	1734-1877	138-281

CHAPTER 3- LONG-TERM FRESHENING OF THE COASTAL YUCATAN AQUIFER SINCE THE MID-HOLOCENE: IMPLICATIONS FOR GROUNDWATER POTABILITY THROUGH THE TERMINAL CLASSIC

Authors: Anya Krywy-Janzen[a*], Eduard Reinhardt[a], Chelsi McNeill-Jewer[a]

[a] McMaster University, School of Geography and Earth Sciences, Hamilton, Ontario, L8S 4K1, Canada

[*] Corresponding author at: McMaster University, School of Geography and Earth Sciences, Hamilton Ontario, L8S 4K1, Canada. Email address: krywyja@mcmaster.ca

3.1 Abstract

The Classic Maya civilization in the Yucatan Peninsula experienced a disintegration of population throughout the Terminal Classic. This decline in population is postulated to have occurred spatially through three phases: the western lowlands at 810 AD, the southeastern lowlands at 860 AD, and lastly, the central and northern lowlands at 910 AD. Many paleoclimate records have hypothesized drought as a cause for this deterioration alongside a variety of other factors. Simultaneously however, a shift towards prosperity in the North and continuation of coastal communities is seen to occur. Understanding the quality of groundwater resources during this time is critical to interpreting these spatial disparities. Four sediment cores retrieved from the Actun Ha cave system (10km from the

Atlantic Ocean) provide records of past climate and groundwater conditions through microfossil and micro X-Ray Fluorescence data. Three cores were taken across the open water cenote at 4-5m water depth with the fourth core taken within the downstream cave passage at a depth of 16m. Sediment accumulation rates and records of Ti, Fe and K were used to indicate changes in the distribution of sedimentation within the cave passages and cenote. The Cl^- record was used alongside the record from the Yax Chen cave system to determine spatial and temporal groundwater conditions. The cenote was seen to flood by 4.3 ka yrs BP and cause the onset of sedimentation within the cave. The coastal groundwater was seen to freshen throughout the Holocene, with a large reduction in salinity occurring through the Terminal Classic. This timing of freshening indicates that populace along the coast may have had access to potable groundwater, giving reason to their continuity.

3.2 Introduction

3.2.1 Classic Maya Decline

The decline of the Classic Maya is a heavily studied phenomenon as it represents a large loss of population and culture. This decline and its relationship with widespread pervasive drought is a prominent point of discussion as it has important implications for how modern demographics could be affected by future climate change. Multiple causes for the decline have also been proposed (warfare, storms, volcanic eruptions and deforestation), but climate change has prevailed as a dominant trigger (Brenner et al,

2002; McNeil et al, 2010; Kennett et al, 2012; Medina-Elizalde et al, 2016; Nooren et al, 2017). Numerous paleoclimate studies have found paleoclimatic evidence for periods of drought during the Terminal Classic, typically focusing on inland sites (Hodell et al, 1995; Curtis et al, 1996; Haug et al., 2001; Hodell et al, 2005; Medina-Elizalde et al, 2010; Kennett et al, 2012) and recent studies have attempted to quantify the impact on freshwater resources to the Maya (Evans et al., 2018; McNeill-Jewer et al., in prep.). Gill et al (2007) proposed that the Mayan population declined spatially and temporarily in three phases: the western lowlands at 810 C.E., the southeastern lowlands at 860 C.E. and lastly, the central and northern lowlands at 910 C.E. A number of the cites affected were home to upwards of 50,000-120,000 people and were located in the southern interior of the Yucatan Peninsula (Masson, 2012). Through this time, a shift towards prosperity in the north was seen to occur alongside survival of smaller coastal towns until the arrival of the Spanish (Dahlin, 2002; Masson, 2012; Jaijel et al., 2018). As access to potable water resources would have been an important aspect of survival through the Terminal Classic, determining the sources and quality of freshwater resources is thus important in the endeavour, and yet there are few studies documenting the changes in the Mayan aquifer and its relationship to these droughts.

3.2.2 Yucatan Hydrology

The Yucatan Peninsula is a large limestone carbonate platform that formed during the Cenozoic (Ward et al., 1985). The region is significantly karstified due to mixing-zone

hydrology, littoral processes and glacioeustacy, which has led to numerous cave systems, dissolution lakes and sinkholes (Beddows, 2004; Smart et al., 2006). These features allow for direct access to ground water and direct infiltration of precipitation through the limestone into the aquifer. The aquifer of the peninsula is unconfined and stratified by temperature and density; a light meteoric water mass overlies a warmer, denser marine water mass that intrudes from the coast (Beddows et al., 2007). A mixing zone, or halocline, separates these water masses, the depth of which increases, with thickness decreasing as distance from the coast increases (Kovacs et al., 2017; Beddows, 2004; Smart et al., 2006). These two water masses are very distinct, the meteoric water mass has a salinity of 1-7 ppt and average temperature of ~25°C, the marine has a salinity of 35 ppt and average temperature of ~27°C (Stoessel, 1995; Stoessell and Coke, 2006). The salinity of the meteoric water mass has been found to increase coastward (Kovacs et al., 2017). Due to connectivity of the aquifer to the ocean through the highly porous karst, flooding of the karst has occurred with Holocene sea-level rise (Gabriel et al., 2009; Collins et al., 2015b; Krywy-Janzen et al., in prep.).

Within Yax Chen cave system, it was found through both uXRF Cl^- and microfossil records that the aquifer has experiencing a freshening over the past ~ 4 ka coincident with increasing arid conditions in the Yucatan (Chan 2017). The decrease in salinity was due to less entrainment of marine water into the meteoric water mass with the reduction of flow. Similarly, Kovacs et al. (2017) found a similar relationship in Hoyo Negro which is a further inland cenote and part of the Sac Aktun cave system. During wet periods, increased

frequency and magnitude of large rainfall events (esp. hurricanes) causes increased meteoric water flow towards the coast which causes entrainment of underlying marine water and thus salinity. This process has also been documented in environmental monitoring studies capturing this effect over several years and spatially from coastal to further inland sites (Kovacs et al., 2018; Kovacs et al., 2017b; Coutino et al., 2017). Coast proximal sites experienced large changes in salinity vs inland sites where the salinity change was smaller in magnitude (Kovacs et al. 2018) This salinity response is due to proximity to the halocline which is at increasing depth moving inland, and also due to the sum of collective mixing as the water flows towards the coast (Kovacs et al., 2018; Kovacs et al., 2017b; Coutino et al., 2017).

3.2.3 Yucatan Paleoclimate Records

The Yucatan Peninsula has a tropical climate with seasons and precipitation determined by the position of the Intertropical Convergence Zone (ITCZ; Hastenrath and Polzin, 2013; Schneider et al., 2014). Yearly, approximately 550-1500 mm of precipitation occurs on average (Bauer-Gottwein et al., 2011). The ITCZ moves south through December to April which causes a dry season with <100mm of precipitation per month (Negreros-Castillo et al., 2003). On the contrary, when the ITCZ moves farther north through May to November, the wet season occurs with increased precipitation levels (Hastenrath and Polzin, 2013). Tropical storms and hurricanes are known to make landfall on the peninsula during the west season. These large rainfall events can cause increased water level and

changes in aquifer salinity through mixing of the meteoric and marine water masses (Kovacs et al., 2017b; Coutino et al., 2017).

Paleoclimate records have been collected at various locations throughout the Yucatan Peninsula and surrounding Caribbean area using a variety of proxies to determine changing Holocene precipitation patterns. These sites include Laguna Chumkopo, the Cariaco Basin, Punta Laguna, Chichancanab and the Yok Balum and Chaac speleothems.

McNeill-Jewer et al (in prep.) used Laguna Chumkopo and Pac Chen Lake cores with high resolution uXRF core scanning using Cl^- values to document past water body salinity changes over the past ~ 4 ka. The analysis found porewater Cl^- preserves past salinity of the water body during sediment deposition and thus changing Evaporation/Precipitation (E/P). Increases in Cl^- were observed at various periods, but especially during the Terminal Classic, coinciding with the Classic Maya droughts. Part of this study also developed a salinity calibration equation for the relationship between Cl^- values from uXRF analysis (counts) and water salinity (ppt). Short cores were collected from various locations spanning different water salinities that were measured using a conductivity sensor allowing the Cl count data to be related to salinity (ppt) with a high degree of confidence (r^2=0.89). Salinity based on this relationship can thus be calculated using the following equation:

$$\text{Salinity (ppt)} = 0.0019(Cl^- \text{ total counts}) - 0.27024$$

Sediment density and thus the gypsum was used in sediment cores from Lake Chichancanab to infer water loss (Hodell et al., 2005). The record from Punta Laguna used δ^{18}O values from benthic ostracods, whereas the speleothem records measured δ^{18}O values from microsamples of layered calcite (Curtis et al., 1996, Medina-Elizalde et al., 2010; Kennett et al., 2012). These δ^{18}O values were used to indicate wet and dry conditions as the δ^{18}O/δ^{16}O ratio of water is controlled by evaporation/precipitation (E/P) regimes with larger δ^{18}O values indicating higher E/P. Understanding of climatic conditions throughout the Holocene, and especially the Terminal Classic Period is furthered by comparing similarities between these records. The relationship between climate change and the Classic Maya has been debated at length, with an increasing number of records being published (Curtis et al., 1996; Haug et al., 2001; Hodell et al., 2005; Medina-Elizalde et al., 2010; Kennett et al., 2012; Douglas et al., 2015). An increase in temporal and spatial resolution is necessary to fully understand this relationship and porewater Cl can offer a sensitive an broadly applicable proxy for E/P in lakes and for groundwater (Chan, 2017; McNeill-Jewer et al., in prep**.;** Kovacs et al., 2017)

3.2.4 Aktun Ha and Yax Chen Cave System

Cenote Carwash and the Aktun Ha cave system are located ~ 8.5 km from the Caribbean coast and northwest of the town of Tulum (Fig. 1). The cenote has a surface area of ~ 1000 m^2 and an average depth of 4m with entrances to the cave system on the

northwest and southern ends (Fig. 2 and 3). Water level is approximately equal to mean sea level with a hydraulic gradient that has previously been measured to be within a range of 6-15cm/km (Beddows, 2004, Gondwe et al., 2010; Moore et al., 1992). The cave passages are mostly shallow and flooded by the meteoric water mass (MWM) with a salinity of 1.4 ppt. At -21 m there is a sharp halocline where the salinity changes to 35.6 ppt (Fig. 4; van Hengstum et al., 2008; Kovacs et al., 2017). Carwash has been studied previously for its connection with sea-level rise, foraminifera and testate amoebae distributions within caves, evolution of aquifer salinity, phytoplankton and use as a drinking source (Alcocer et al., 1998; Gabriel et al., 2008; Sanchez et al., 2002; van Hengstum et al., 2008; van Hengstum et al., 2009; van Hengstum et al., 2010).

Yax Chen is ~ 300m from the Caribbean coast and just south of Tulum (Fig. 1). The cave system is a part of the larger Ox Bel Ha network and consists of ~ 2.7 km of explored conduits with seven cenotes along the main cave line (see Fig. 2 in Collins et al., 2015b). The cave passages are fairly shallow at ~ 10 to 14 m depth and were seen to flood alongside Holocene sea-level (Collins et al., 2015b). As the cave system is right on the coast, it has a stepped halocline at ~ 10 - 11 m and ~ 15 m depth (Kovacs et al., 2017a). The Yax Chen cave system has been used to study the relationship between aquifer elevation and sea-level, hydrological and sedimentological response to hurricanes, and long-term (~ 4 ka) salinity changes of the aquifer and its relationship with climate and the Classic Maya Droughts (Collins et al., 2015a; Collins et al., 2015b; Coutino et al., 2017; Kovacs et al., 2017b; Chan, 2017).

3.2.5 µXRF Core Analysis

µXRF core scanning is a noninvasive method of elemental analysis at a resolution of up to 200 µm within sediment cores (Croudace and Guy Rothwell, 2015). Using an external X-ray source to strike sediment causes an emission of x-radiation (XRF), with each element producing a characteristic X-ray fluorescence spectrum. This is what allows the measurement of elemental composition of sediment to be possible. As the method is noninvasive, it allows for the preservation of sediment cores. Titanium, iron and potassium have been previously used in sediment as indicators of a terrigenous input and thus increased precipitation (Haug et al., 2003; Gregory et al., 2015; Chaugue-Goff et al., 2016). These terrigenous products are created when rock, regolith and soil undergoes weathering which is transported as soluble ions and insoluble particles (eg., oxyhydroxides) via surface runoff into the water body, or in the case of the highly porous karst of the Yucatan, through the subsurface to the aquifer. However, there may be lags in the response of this weathering process that may not detect short term changes, but does show broad patterns of wet and dry conditions (Krywy-Janzen et al., this volume). Chlorine has been used a proxy of changes in porewater salinity through evaporation regimes as it represents the presence of chloride ions in the water body during deposition of the sediment (Kovacs et al., 2017a; Peros et al., 2017; Chan, 2017; McNeill-Jewer et al., in prep.). During high E/P periods water salinity would be elevated, and thus would have higher Cl, vs lower E/P and lower Cl. In the case of groundwater, where there is negligible

evaporation, the Cl measures mixing between the meteoric and marine water masses (Kovacs et al., 2017a; Chan, 2017). Similarly, Cl and Br were used to identify periods of drying and increased evaporation during the 8.2 Ka dry event in Cenote Jennifer, Cuba (Peros et al., 2017). Cl/Ca was used with Sr/Ca in calcite raft cores from Hoyo Negro and Ich Balam, Mexico, to document decreases in aquifer salinity through drying climate trends over the past 8 ka (Kovacs et al., 2017a). Most recently, Cl has been used to document and quantify increases in aquifer salinity due to climate through the Terminal Classic in Laguna Chumkopo, Mexico, as well as freshening of the Yax Chen cave system, Mexico, due to drying climate (Chan., 2018; McNeill-Jewer et al., in prep.). Ca is used as an indicator of carbonate content which can be related to water body characteristics and biological productivity (Foerster et al., 2012; Krywy-Janzen et al., this volume). Incoherent/Coherent is used as an indicator of organic/water content in sediment (Jouve et al., 2013). Incoherent values represent the incoherent or Compton scattering and coherent values represent the Raleigh scattering. Ratios of these values (Inc/Coh) is inversely proportional to the average of the atomic weight, which is why it is representative of the amount of organic/water content.

3.2.6 Foraminifera and Testate amoebae in Anchialine Cave Systems

Foraminifera and testate amoebae (arcellaceans), are useful as paleoenvironmental proxies as they inhabit almost all aquatic environments and are very responsive to changes in salinity, temperature and pH (Scott et al., 2001). Both taxonomic

groups are typically well-preserved in the sediment record as they form simple secreted or agglutinated tests. Foraminifera are typically found in marine to brackish environments (ex. ocean and upper salt marshes), whereas testate amoebae inhabit freshwater to slightly brackish environments (ex. lakes, bogs salt marshes and soil) and both experience ecological zonation in response to their environment (Scott et al., 2001; Patterson and Kumar, 2002; Murray, 2006). Within the Yucatan Peninsula, microfossils have been used to determine changes in aquifer condition (paleohydrology) and sea-level as salinity is a dominant control on their distribution (Gabriel et al., 2008; van Hengstum et al., 2008, van Hengstum et al., 2009; van Hengstum et al 2010; Chan et al., 2018). van Hengstum et al (2008) found that within cenotes, assemblages shift from testate amoebae-dominated to foraminifera-dominated above ~3.5 psu and that anchialine cenotes are one of the few environments where testate amoebae and foraminifera can coexist, and the collective ecology can be studied. In both Runway Sinkhole, Bahamas and Cliff Pool Sinkhole, Bermuda, *Physalidia simplex* were observed, amongst other species, as an indicator of the onset of anchialine conditions when looking at environmental changes in both systems (van Hengstum and Scott, 2011; Kovacs et al., 2013).

3.3 Methods

3.3.1 Sediment Cores

Two push cores were retrieved from Carwash using self-contained underwater breathing apparatus (SCUBA). C5 was collected at the downstream cave entrance at a depth of 4.6

m and was 57 cm long. C6 was collected at the upstream cave entrance at a depth of 5.6 m and was 66 cm long. C1 and C2 were retrieved for previous studies also using SCUBA (Gabriel et al., 2009; van Hengstum et al., 2010). C1 was collected near the south-end of the cenote at a depth of 4 m and was 61 cm long. C2 was collected in the downstream cave at a depth of 16 m and was 50 cm long (Fig. 2 and 3). Core depths were recorded using a calibrated depth gauge and are relative to local water level, and core locations were referenced using the baseline for the mapping survey (see 3.3.2).

Core elemental analysis was conducted using a Cox Analytical Systems Itrax XRF core scanner at the McMaster University Facility. Analysis used the Chromium heavy element (CR-HE) X-ray source (30 kv, 10 mA, exp. time = 15 sec, step-size = 500µm). C5 and C6 were analyzed intact, but C2 which had been previously sampled at centimeter intervals was analyzed using the Sequential Sample Reservoir (SSR) and measurements from each reservoir were averaged after analysis (Gregory et al., 2017).

Microfossil analyses from C1 and C2 are outlined in their respective studies (Gabriel et al., 2009; van Hengstum et al., 2010). In this study, sediment samples (~ 1.25 cm^3) from C5 and C6 were wet sieved using a 45 µm screen. Samples were then wet-split and identified using standard procedures and taxonomy (Medioli and Scott, 1983; Scott and Hermelin, 1993; Scott et al., 2001; van Hengstum et al., 2008, van Hengstum et al., 2009; van Hengstum et al 2010). Species distributions are shown as percent (%) of the total microfossil abundance unless otherwise noted.

Five radiocarbon samples were obtained from C5 and C6. Samples were twigs and undifferentiated organic matter (OM) and sent to A.E. Lalonde AMS Laboratory and analyzed with a 3MV tandem accelerator mass spectrometer. The R statistical software package Bacon 2.3 (Balauw and Christen, 2011) was used with the northern hemisphere calibration curve IntCal13 (Reimer et al., 2013) to calibrate raw radiocarbon ages as ranges in calibrated years before present (cal yrs BP) with a 95% confidence interval. An age model was fit to the data and interpolated ages throughout both cores were calculated every 500 µm to match with XRF core measurement resolution. Cited radiocarbon ages are in cal yrs BP unless otherwise noted.

3.3.2 Cenote Mapping

A depth profile and map for Carwash were created using depth and distance data from a survey taken by Mexico Cave Exploration Project (MCEP) divers in May of 2017. A base line was laid on the cave bottom using tie-offs on rocks at various points. Distance and azimuth was then measured to each of these tie-offs of the baseline. Sidewall, bottom and ceiling measurements were then collected at tie-off points along this baseline using a combination of tape measure and depth gauge (± 0.1 m). The baseline extend through the open water of the cenote and 30-40m into the upstream and downstream cave passages.

3.4 Results

3.4.1 Stratigraphy/Age Models

All radiocarbon dates occurred chronologically, and there were no age reversals within the cores (Fig. 5; Table 1). The age model of C5 showed to be very similar to that of C1 which was collected previously with an interpolated basal age of ~7000 years BP, ~ 300 years less than that of C1 (Gabriel et al., 2009). Sedimentation is considerably high throughout almost the whole core, until the top 5 cm where sedimentation slows and represents the last ~6000 years of sedimentation. C2 has a stepped accumulation record with periods of high and low sediment accumulation, whereas C6 has a more consistent accumulation. Both cores span ~ 4000 yrs of depositional history.

The majority of C5 is composed of dark, organic-rich peat with whole and fragmented gastropod shells and plant matter occurring throughout (Fig. 6). C6 is more variable, with layers of lighter sediment and gastropods interspersed with darker, more organic rich layers (Fig. 8). Gastropods occur in smaller amounts throughout the core with seeds, small twigs and undifferentiated OM.

3.4.2 Microfossils

In C5, two species of testate amoeba (*Centropyxis aculeata* and *Centropyxis constricta*) and one species of foraminifera (*Physalidia simplex*) were found, but only in the top 0 - 4 cm. Ostracods, *Cytheridella ilosvayi* and *Darwinula stevensoni* were found throughout the core. These results are similar to those of C1 analyzed by Gabriel et al

(2009; Fig. 7). The diatom *Terpinsoë musica*, was also observed to be in the upper 0-4 cm, but not present in the lower portion of the core. This diatom has previously been found in Mexico, typically in freshwater habits although it can inhabit a range of environments (Carmona Jimenez et al., 2017).

In C6, the same testate amoebae and foraminifera were found but also *Arcella vulgaris*. These taxa were found throughout the core as it spans the last ~ 4000 yrs and thus is equivalent in age to the very upper portion of C1 and 5. The distribution of *Centropyxis* spp. is relatively continuous throughout the core, with *C. aculeata* being the most dominant varying between ~ 50 - 60 %. *P. Simplex* however, is more abundant at the base of the core (~ 10 - 30%) with a notable reduction between 45 - 55 cm. *Terpinsoë musica*, was also observed throughout the whole core.

3.4.3 uXRF Data

Terrigenous element counts (Ti, K and Fe) in C5 are fairly consistent (~ 0 - 100, 0 - 200, 50 - 200) until the top 4 cm, where a they increase (> 250) along with the microfossil abundance as discussed previously (Fig. 5, 6). Cl shows a similar trend not varying greatly but showing slightly larger values between 0 - 4 cm (~ 750 - 1000 vs >1000). Inc/Coh and Ca covary but are largely unchanging through the length of the core and follow changes in carbonate content of the sediment (i.e. ~ 30 cm; Fig 5).

In C6, there is a larger variation with all elemental records and visually appears to have larger variations in lithology, but the Ca and Inc/Coh values are fairly consistent

throughout other than a few shell (~ 48 - 55 cm) concentrations and a stick (~ 18 - 23 cm) where Ca increases and decreases respectively (Fig. 8). Terrigenous element counts (Ti, K and Fe) in C6 are fairly consistent (~ 0 - 100, 0 - 200, 50 - 200) with some large increases that appear matrix related, but there is little change in Coh/Inc over the same intervals (esp. Fe). These values are quite similar to the majority of the record from C5 excluding the top 0 - 4 cm where these values are higher. The Cl record in C6 has an overall decreasing trend up core going from ~ 1000 at the base to ~ 500 at the top, with large rapid spikes in values (> 1500) throughout the core, but they also tend to me more prevalent in lower parts of the core. There aren't any matrix effects with the Cl records as there is with then terrigenous elements. Cross-plots of terrigenous elements and Inc/Coh values with the Cl shows no discernible relationship. There is also good agreement between Cl values and *P. simplex* (%) in C2 and C6 which is sensitive to salinity as discussed previously. *P. simplex* will typically start to disappear from the record when salinity is below 3.5 ppt and completely disappear below 1 ppt (van Hengstum et al., 2008). The Cl values are higher in C2 versus C6, but this is predicted, as C2 (-16 m) is closer to the halocline (-21 m) and thus will record larger salinity changes, while C6 which is at a higher elevation (-5.6 m) within the meteoric water mass.

3.5 Discussion

3.5.1 Site Evolution

Data from previous cores taken in the cave passage (C2) and cenote (C1) with cores from this study (C5, C6) were used to determine site evolution which is also partly described in Collins et al, (2015b) and Gabriel et. al. (2009) but without this new data (Fig. 12).

3.5.1.1 No Connection

At ~ 9000 years BP sea-level was ~ 14 m MSL (meters below modern sea-level) based on the Khan et al (2017) sea level curve, shallowly flooding the deeper cave passages connected to Carwash. None of the collected cores have records that extend back this far. The depth of the cave passage at C2 is -16 m and based on Holocene sea-level it should have been flooded by 9000 yrs BP, but the basal age is 4300 yrs BP, indicating sedimentation didn't start with initial flooding because there was no source, or input of sediment until water level was at a higher elevation (Collins et al., 2015). This is a common phenomenon in the caves of the Yucatan, where even today, there is no sediment deposition even after the cave passages have been flooded for thousands of years. As there was no open water aquatic environment in the cenote, nor a connection between upstream and downstream cave passages to allow flow and movement of sediment, it is not surprising that there is no sediment record of the initial flooding of the cave passage.

3.5.1.2 Limited Connection

The second phase occurs at ~6500 years BP when water has risen to ~ -4 m MSL close to the top of the breakdown pile in the cenote forming a mangrove. This is represented in C1 and 5 as organic rich peat throughout most of the cores. Gabriel et al (2009) found this peat contains *R. mangle* (red mangrove) pollen, indicating shallow water conditions that allowed these mangroves to grow on the cenote breakdown pile. Little terrigenous input is reaching the mangrove as Ti, K and Fe are relatively low (Fig. 6). Runoff would have been reaching the cenote, but not necessarily reaching the mangrove pile in the middle due to step sided topography of the cenote and low water level. The sediment accumulation rate of C1 and C5 indicate that most of the detrital OM was being trapped in the mangrove topography of the breakdown pile. Sediment would be accumulating and building up in the lower spaces between breakdown boulders infilling that topography (Fig. 12).

3.5.1.3 Shallow to Full Connection

The third phase occurs at ~4300 years BP where water level is ~3 m MSL based on the Holocene sea-level record which had flooded the breakdown pile at -5.6 m. At this point, there is an open body of water ~ 2.5 m deep in the cenote allowing connection between the upstream and downstream cave passages and is the point in time sediment begins to accumulate in C2. Because there is now sunlit open water areas, primary

productivity can now occur in the cenote and move sediment into the downstream cave passage with aquifer flow which continued with Holocene sea-level rise (Khan et al., 2017)

Sedimentation during the mangrove phase (~ 6000 yr BP) had infilled much of the boulder topography producing a flat planar surface that prevented sediment deposition in much of the area. In C1 and C5, the < 6500 yr BP depositional record is represented by ~ 4 cm. Terrigenous elements (Ti, K, Fe) have higher values in this interval, because runoff from the surrounding karst could now be widely distributed in the open water body of the cenote. However, the higher Ti, K, Fe values could also be due their concentration in the sediment with the low accumulation of OM and its quick decay.

C1 and C5 were collected on the flat bottom of the cenote, but C6 which records the last ~ 4 ka, was collected at a slightly deeper depth (-5.6 m) and on the side of the breakdown pile. This depression had not infilled with mangrove sedimentation, so sediment was preferentially accumulating here, and in other depressions after ~ 6500 yrs BP. The core did not reach refusal, which is likely why we only have the last 4 ka of deposition.

3.5.2 Comparison of Yax Chen and Carwash Chlorine Records

The Carwash (C6) and Yax Chen (C3) Cl records spanning the last 4 ka show very good correspondence, with an overall decreasing trend, but also shared perturbations from that trend albeit at different magnitudes. The Cl count data in Yax Chen is ~ 6000 - 10000 compared to Carwash which is ~ 300 - 1500, and based on the salinity calibration

this represents ~ 5 ppt of variation versus 1-2 ppt in Carwash (Chan 2017; Fig. 13). These salinities fit with the instrumentally observed seasonal salinity change due to large rainfall events (i.e. tropical storms, hurricanes) in Yax Chen itself (~ 5 ppt), and other inland sites like that of Carwash (<1 ppt; Kovacs et al 2017b; Kovacs et al., 2018). The magnitude of Cl variation in the water column at any given location is partially a function of the vertical distance of the core site from the halocline, but also its distance inland. Chan (2017) noted differing Cl records in Yax Chen cores depending on their depth and thus proximity to the halocline. Cores close to the halocline (< 0.5 m) showed larger fluctuations of Cl due to entrainment of marine water into the meteoric water mass and seasonal movement of the halocline, but cores further away from the halocline showed overall changes in salinity of the meteoric water mass (Fig. 11). Yax Chen C3, which is used for comparison here, was collected at ~ 9 m depth and was deemed to be far enough away from the halocline (-11 m) that it would primarily record overall meteoric water mass salinity (Chan, 2017). Carwash is much further inland (8.5 km vs 0.3 km) and C6 (-5.6 m) is further away from the halocline (-21 m) than C3 in Yax Chen, so it would be expected to have smaller salinity variations which is the case. In Carwash itself, we see this relationship with the halocline as well, since C2 has higher Cl values because it is < 5 m away from the halocline versus C6 which is ~ 15 m, but both locations showed similar trends in Cl through the last 4 ka, albeit of different magnitudes. The Cl record in Yax Chen will be more extreme in terms of fluctuations vs inland sites like Carwash because meteoric salinity in Yax Chen will be the result of successive entrainment events as meteoric water flows to the coast (Fig. 11;

Coutino et al., 2017). The magnitude of that entrainment of marine water into the meteoric water mass would also increase moving coastward as the halocline became shallower.

3.5.4 Comparison to Other Climate Records

The Cl records spanning the last 4 ka from Holocene from Carwash and Yax Chen show good correspondence with temperature reconstructions from Greenland as well as Bond events and cold/dry events indicating a teleconnection between changes in the aquifer and global climate cycles (Fig. 13 and 14). Greenland surface temperature is a key constraint for the mass of the Greenland ice sheet, and in turn global sea-level and ocean circulation as these reconstructed surface temperatures are not subject to seasonal temperature swings (Hanna et al., 2008; van den Broeke et al., 2009; Kobashi et al., 2011). Bond cycles are oscillations during the last Ice Age, where cold, ice-bearing surface waters were advected southward and eastward into warmer waters (Bond et al., 2001). Through the Holocene, warm and stable climate was interrupted by six cold events within the Northern Hemisphere, during which the poles were cool and the tropics were dry (Mayewski et al., 2004; Wanner et al., 2011). These events were recreated using over 100 studies postulating signals of Bond events, temperature proxies, glacier reconstructions and humidity/precipitation proxies, including the Chichancanab and Cariaco Basin records (Haug et al., 2001; Hodell et al, 2005). A cold/dry period was defined by Wanner et al. (2001) to be a period of time when the temperature or humidity/precipitation proxy

values used fell below one half of the standard deviation of the Holocene mean value. These events were found to occur due to three forcing mechanisms (orbital, solar and volcanic), the variation and extent of each mechanism changing over time (Wanner et al., 2008). The cold events at 2700 and 550 yrs BP all line up with very distinct decreases in salinity in both Cl^- records as well as the records from Laguna Chumkopo and Lake Chichancanab (Fig. 13; Hodell et al., 2005; McNeill-Jewer et al., in prep.). Hydrology within the Yucatan is responding to these drying events and undergoing drying as well, as seen in freshening of the aquifer during these times. Although the records aren't perfectly corresponding to the event at 1550 yrs BP, this may be due to radiocarbon dating resolution or small changes within the global climate might not correspond to a large response within the aquifer. Peros et al (2017) documented a response in the Cuba during the cold/dry period that occurred 8.2 ka, further proving that these events are being recorded in the Caribbean. When comparing the records to average temperatures in Greenland through the same period of time, the records show very similar trends (Kobashi et al., 2011). Greenland temperatures are also showing a general decreasing/cooling trend towards the present with distinct decreases of ~2 °C at the same times as both Cl records (800-700 B.C.E. and 700-900 C.E. most markedly; Fig. 14). This correspondence is excellent as we would be expecting that cold periods in Greenland (the poles) would line up to dry periods in Mexico (the tropics). Cl^- is responding to global climate events, proving that not only local factors are causing changes within the hydrology of the Yucatan aquifer. As global changes in temperatures have an effect on flow and salinity within the

aquifer, it is very probable that increasing global temperatures will cause more precipitation events within the tropics, leading to increased salinity within the coastal Yucatan aquifer.

3.5.4.1 2.7-2.5 ka Event

The cold/dry event that occurred at 2.7-2.5 ka has been postulated to be a plausible forcing of solar variability (Mayewski et al., 2004; Wannar et al., 2008). During this time, we see a very pronounced change in paleoclimate records from the Yucatan (Fig. 13 and 14). Carwash and Yax Chen show ~1 and 5ppt decreases in salinity, respectively, for >200 years. Laguna Chumkopo experiences spikes in Cl^- that are much more condensed than those during the Maya droughts (McNeill-Jewer et al., in prep.). Lake Chichancanab records a spike in sediment density that is approximately 1.6 g/cm3 and comparable to those recorded during the Maya droughts, indicating an extremely dry period as these horizons are only recorded once the evaporitic threshold for gypsum is reached (Hodell et al., 2005). Based on all of these records, the Yucatan Peninsula is experiencing a fairly extreme dry period. When referencing archaeological events, the first culturally Maya peopling of the Northern Yucatan Peninsula occurred at this time, specifically the northern and southern lowlands (Rissolo et al., 2005; Glover et al., 2011). This cold/dry event has yet to be recognized within Yucatan paleoclimate records, and based on the archaeology, has potentially important implications for peopling of the Yucatan that need to be further investigated.

3.5.4.2 Comparison to Maya Terminal Droughts

By converting the chlorine records from Carwash and Yax Chen to salinity (ppt) the effect on freshness can be quantitatively observed (McNeill-Jewer et al., in prep.). These records have been compared to other paleoclimate records in the region and the timeline of the Maya civilization and show a freshening or drying trend during the same time as the Maya Terminal Droughts at ~750-900 C.E. (Fig. 13; Curtis et al., 1996; Haug et al., 2001; Hodell et al., 2005; McNeill-Jewer et al., in prep.). Although both records are showing freshening trends throughout the Classic, they undergo a prominent decrease of ~1ppt in Carwash and 5ppt in Yax Chen in salinity over 300 years that coincides with the Terminal Classic but with larger variation occurring and showing small periods of increase in salinity. As our records show higher resolution (500µm), it makes sense that both Cl records would show higher variability than the other records that sample on as low as a 1cm scale. This is conducive with the hypothesis of alternating dry and wet periods during this time (Hodell et al., 2005; Medina-Elizalde et al., 2010; Douglas et al., 2015). The records from Chumkopo and Chichancanab show this similar variation during the Terminal Classic through as well as stabilization in values directly after (Hodell et al., 2005; McNeill-Jewer et al., in prep.). These droughts do not appear to be impacted by global climate or Bond cycles as they don't line up with any recorded, however, they do line up with a distinct decrease in Greenland temperature (Fig. 14).

3.5.5 Implication for Survival of Maya Through Terminal Classic

With freshwater resources becoming increasingly limited throughout the Terminal Classic, location and abundance of these resources would have determined locality of the Maya. Surface water shows the most freshening and potential for being potable through the Terminal Classic, therefore access to cenotes and other groundwater sources, which largely exist along the coast, would have had a large implication for where people were living. These sources are typically easily accessible but are not huge water bodies and therefore not able to support large populations. Even though the record from Yax Chen shows that it was not potable, Cenote Carwash is almost 10km from the coast and shows the same trends. Based on this reproducibility, it is possible that other cenotes close to the coast would have gone through an almost identical freshening. If the upper meteoric water mass in these sources was potable through the Terminal Classic, we think this may have implications for the patterning of population decline and survival of coastal communities during this time. Further work needs to be done with a variety of spatial groundwater resources along the Yucatan coast to constrain the potability of these resources during the Terminal Classic.

3.6 Conclusions

The paleoenvironment record from Cenote Carwash shows flooding of the aquifer alongside sea level rise as well as a decrease in storminess and long-term freshening of

the coastal aquifer through the Holocene. The Cl^- record further proved its usefulness as a proxy as it documented a wide variety of events in terms of time-range and scale that occurred regionally throughout the aquifer as seen with the reproducibility of the record within Yax Chen. Large freshening periods coincided with global col/dry events revealing hydrological response to global climate cycles. The largest period of freshening occurred during the Terminal Classic period, supporting the hypothesis of drought-like conditions. Freshening of the coastal aquifer caused the upper meteoric water mass to become potable during this time, which may have attributed to the continuation of Maya communities along the coast. Further determining which water resources along the coast were potable through the Terminal Classic will help constrain understanding of the spatial survival of the Maya.

3.7 Acknowledgements

The authors would like to thank Zero Gravity Dive shop and the Mexican Cave Exploration Project for dive support and logistics. Special thanks to Hildegarden Wiggenhorn, Peter Gaertner, Sven Nellers and Mike Schernbeck for conducting the cave survey of Carwash. Funding was provided by National Sciences and Engineering Research Council of Canada (EGR-Discovery).

3.8 References

Alcocer J., Lugo A., Marin L., and Escobar E. (1998) Hydrochemistry of waters from five cenotes and evaluation of their suitability for drinking-water supplies, northeastern Yucatan, Mexico. *Hydrogeology Journal* **6**, 293-301.

Bauer-Gottwein P., Gondwe B., Charvet G., Marin L., Rebolledo-Vieyra M. and Merediz-Alonso G. (2011) Review: The Yucatán Peninsula karst aquifer, Mexico. *Hydrogeology Journal* **19**, 507-524.

Beddows P. (2004) Groundwater hydrology of a coastal conduit carbonate aquifer: Caribbean coast of the Yucatán Peninsula, México (Doctoral dissertation, University of Bristol).

Beddows P., Smart P., Whitaker F., Smith S. (2007) Decoupled fresh-saline groundwater circulation of a coastal carbonate aquifer: Spatial patterns of temperature and specific electrical conductivity. *Journal of Hydrology* **346**, 18-32.

Blaauw, M., and Christen, J.A. (2011) Flexible paleoclimate age-depth models using an autoregressive gamma process. *Bayesian Analysis* **6**, 457-474.

Bond G., Kromer B., Beer J., Muscheler R., Evans M., Showers W., Hoffman S., Lotti-Bond R., Hajdas I. and Bonani G. (2001) Persistent solar influence on North Atlantic Holocene climate during the Holocene. *Science* **294**, 2130-2136.

Brenner M., Rosenmeier M., Hodell D. and Curtis J. (2002) Paleolimnology of the Maya Lowlands: Long-term perspectives on interactions among climate, environment, and humans. *Ancient Mesoamerica* **13**, 141-157.

Carmona Jimenez J., Beltran Magos Y. and Salinas Camarillo V.H. (2017) Morphological and environmental characterization of Terpsinoë musica (Biddulphiaceae, Bacillariophyceae) in tropical streams from Mexico. *Diatom Research* **32**, 185-193.

Chague-Goff C., Chan J., Goff J. and Gadd P. (2016) Late Holocene record of environmental changes, cyclones and tsunamis in a coastal lake, Mangaia, Cook Islands. *Island Arc* **25**, 333-349.

Chan W.M. (2017) Paleohydrologic reconstruction of Yax Chen Cave (Yucatan Peninsula, Mexico) in response to Holocene climate change (Master's Thesis; McMaster University).

Collins S., Reinhardt E., Werner C., Le Maillot C., Devos F. & Meacham S. (2015). Regional response of the coastal aquifer to Hurricane Ingrid and sedimentation flux in the Yax Chen cave system (Ox Bel Ha) Yucatan, Mexico. *Palaeogeography, Palaeoclimatology, Palaeoecology* **438**, 226-238.

Collins S., Reinhardt E., Werner C., Le Maillot C., Devos F., and Rissolo D. (2015) Late Holocene mangrove development and onset of sedimentation in the Yax Chen cave system (Ox Bel Ha) Yucatan, Mexico: Implications for using cave sediments as a sea-level indicator. *Palaeogeography,Palaeoclimatology, Palaeoecology* **438**, 24-134.

Croudace I. and Guy Rothwell R. (2015) Micro-XRF studies of sediments cores: applications of a non-destructive tool for the environmental sciences (developments in paleoenvironmental research). *Tracking Environmental Change Using Lake Sediments. Volume 2: Physical and Geochemical Methods*, 1-464.

Curtis J., Hodell D., and Brenner M. (1996) Climate variability on the Yucatan Peninsula (Mexico) during the past 3500 years, and implications for Maya cultural evolution. *Quaternary Research* **47**, 37-47.

Dahlin B. (2002) Climate change and the end of the classic period in Yucatan: Resolving a paradox. *Ancient Mesoamerica* **13**, 327-340.

Douglas P., Pagani M., Canuto M., Brenner M., Hodell D., Eglington T. and Curtis J. (2015) Drought, agricultural adaptation and sociopolitical collapse in the Maya Lowlands. *Proceedings of the National Academy of Sciences* **112**, 5607-5612.

Evans N., Buaska T., Gazquez-Sanchez F., Brenner M., Curtis J. and Hodell D. (2018) Quantification of drought during the collapse of the classic Maya civilization. *Science* **361**, 498-501.

Foerster G., Junginger A., Langkamp O., Gebru T., Asrat A., Umer M., Lamb H., Wennrich V., Rethemeyer J., Nowaczyk N., Trauth M. and Schaebitz F. (2012) Climatic change recorded in the sediments of the Chew Bahir basin, southern Ethiopia, during the last 45,000 years. *Quaternary International* **274**, 25-37.

Gabriel J., Reinhardt E., Peros M., Davidson D., van Hengstum P., and Beddows P. (2008) Paleoenvironmental evolution of Cenote Aktun Ha (Carwash) on the Yucatan Peninsula, Mexico and its response to Holocene sea-level rise. *Journal of Paleolimnology* **42**, 199-213.

Gill R., Mayewski P., Nyberg J., Huag G. and Peterson L. (2007) Drought and the Maya collapse. *Ancient Mesoamerica* **18**, 283-302.

Glover J., Rissolo D., Ball J. and Amador F. (2011) Who were the middle preclassic settlers of Quintana Roo's north coast? New evidence from Vista Alegre. *Mexicon* **33**, 69-73.

Gondwe B., Lerer S., Stisen S., Marin L., Rebolledo-Vierya M., Merediz-Alonso G. and Bauer- Gottwein P. (2010) Hydrogeology of the south-eastern Yucatan Peninsula: New insights from water level measurements, geochemistry, geophysics and remote sensing. *Journal of Hydrology* **389**, 1-17.

Gregory B., Peros M., Reinhardt E. and Donnelly J. (2015) Middle-late Holocene Caribbean aridity inferred from foraminifera and elemental data in sediment cores from two Cuban lagoons. *Palaeogeography, Palaeoclimatology, Palaeoecology* **426**, 229-241.

Gregory B., Reinhardt E., Macumber A., Nassar N., Patterson T., Kovacs S., and Galloway J. (2017) Sequential samples reservoirs for Itrax-XRF analysis of discrete sample. *Journal of Paleolimnology* **57**, 287-293.

Hanna E., Huybrechts P., Steffen K., Cappelen J., Huff R., Shuman C., Irvine-Fynn T., Wise S. and Griffiths M. (2008) Increased runoff from melt from the Greenland ice sheet: a response to global warming. *Journal of Climatology* **21**, 331-341.

Hastenrath S. and Polzin D. (2013) Climatic variations in Central America and the Caribbean. *International Journal of Climatology* **33**, 1348-1356.

Haug G., Hughen K., Sigman D., Peterson L., and Röhl U. (2001) Southward migration of the Intertropical Convergence Zone through the Holocene. *Science* **293**, 1304-1308.

Haug G., Gunther D., Peterson L., Sigman D., Hughen K. and Aeschlimman B. (2003) Climate change and the collapse of the Maya civilization. *Science* 299, 1731-1735.

Hodell D., Brenner M., and Curtis J. (2005) Terminal Classic drought in the Maya lowlands inferred from multiple sediment cores in Lake Chichancanab (Mexico). *Quaternary Science Reviews* **24**, 413-1427.

Jaijel R., Glover J., Rissolo D., Beddows P., Smith D., Ben-Avraham Z. and Goodman-Tchernov B. (2018) Coastal reconstruction of Vista Alegre, and ancient maritime Maya settlement. *Palaeogeography, Palaeoclimatology, Palaeoecology* **497**, 25-36.

Jouve G., Francus P., Lamoureux S., Provencher-Nolet L., Hanh A., Habberzettl T., Fortin D., Nuttin L. and The PASADO Science Team (2013). Microsedimentological characterization using image analysis and m-XRF as indicators of sedimentary processes and climate changes during Lateglacial at Laguna Potrok Aike, Santa Cruz, Argentina. *Quaternary Science Reviews* **71**, 191-204.

Kennett D., Breitenbach S., Aquino V., Asmerom Y., Awe J., Baldini J., Bartlein P., Culleton B., Ebert C., Jazwa C., Macri M., Marwan N., Polyak V., Prufer K., Ridley H., Sodemann H., Winterhalder B., and Haug G. (2012) Development and disintegration of Maya political systems in response to climate change. *Science* **338**, 788-791.

Khan N., Ashe E., Horton B., Dutton A., Kopp R., Brocard G., Engelhart S., Hill D., Peltier W.R., Vane C. and Scatena F. (2017) Drivers of Holocene sea-level change in the Caribbean. *Quaternary Science Reviews* **155**, 13-36.

Kobashi T., Kawamura K., Severinghaus J., Barnola J.M., Nakaegawa T., Vinther B., Johnsen S and Box J. (2011) High variability of Greenland surface temperature over the past 4000 years estimated from trapped air in an ice core. *Geophysical Research Letters* **38**, L21501, doi:10.1029/2011GL049444.

Kovacs S., van Hengstum P., Reinhardt E., Donnelly J. and Albury N. (2013) Late Holocene sedimentation and hydrologic development in a shallow coastal sinkhole in Great Abaco Island, The Bahamas. *Quaternary International* **317**, 118-132.

Kovacs S., Reinhardt E., Chatters J., Rissolo D., Schwarcz H., Collins S., Kim S.T., Nava Blank A. and Luna Erreguerena P. (2017) Calcite raft geochemistry as a hydrological proxy for Holocene aquifer conditions in Hoyo Negro and Ich Balam (Sac Actun Cave System), Quintana Roo, Mexico. *Quaternary Science Reviews* **10**, 205-214.

Kovacs S., Reinhardt E., Statsna M., Coutino A., Werner C., Collins S., Devos F., and Le Maillot C. (2017) Hurricane Ingrid and Tropical Storm Hanna's effects on the salinity of the coastal aquifer, Quintana Roo, Mexico. *Journal of Hydrology* **551**, 703-714.

Kovacs S., Reinhardt E., Werner C., Kim S.T., Devos F., and Le Maillot C. (2018) Seasonal trends in calcite-raft precipitation from cenotes Rainbow, Feno and Monkey Dust, Quintana Roo, Mexico: Implications for paleoenvironmental studies. *Palaeogeography, Palaeoclimatology, Palaeoecology* **497**, 157-167.

Krywy-Janzen A., Reinhradt E., McNeill-Jewer C., Coutino A., Waltham B., Statsna M., Rissolo D., Meacham S. and van Hengstum P. (2018) Water level rise in Lake Pac Chen, Quintana Roo, Mexico infers connection with the aquifer and response to Holocene sea-level. (Manuscript in preparation).

Masson M. (2012) Maya collapse cycles. *Proceedings of the National Academy of Sciences* **109**, 18237-18238.

Mayewski P., Rohling E., Stager J., Karlén W., Maasch K., Meeker L., Meyerson E., Gasse F., van Kreveld S., Holmgren K. and Lee-Thorp J. (2004) Holocene climate variability. *Quaternary Research* **62**, 243-255.

McNeil C., Burney D. and Burney L. (2010) Evidence disputing deforestation as the cause for the collapse of the ancient Maya polity of Copan, Honduras. *Proceedings of the National Academy of Sciences of the United States of America* **107**, 1017-1022.

McNeill-Jewer C., Reinhardt E., Krywy-Janzen A., Coutino A., Statsna M., Rissolo D. and Meacham S. (2018) Salinity changes during the Maya droughts documented through pore water chlorine in sediment core from Quintana Roo, Mexico. (Manuscript in preparation).

Medina-Elizalde M., Burns S., Lea D., Asmerom Y., Gunten L., Polyak V., Vuille M., and Kalmalker A. (2010) High resolution stalagmite climate record from the Yucatan Peninsula spanning the Maya terminal classic period. *Earth and Planetary Science Letters* **298**, 255-262.

Medina-Elizalde M., Polanco-Martinez J., Lases-Hernandez F., Bradley R. and Burns S. (2016) Testing the "tropical storm" hypothesis of Yucatan Peninsula climate variability during the May Terminal Classic Period. *Quaternary Research* **86**, 111-119.

Medioli F., and Scott D. (1983) Holocene Arcellacea (thecamoebians) from Eastern Canada. *Cushman Foundation Special Publication* **21**, 5-63.

Moore Y., Stoessell R. and Easley D. (1992) Fresh-Water/Sea-Water Relationship within a ground-water flow system, Northeastern coast of the Yucatan Peninsula. *Groundwater* **30**, 343-350.

Murray J. (2006) Ecology and applications of benthic foraminifera. *Cambridge University Press, New York, USA*

Negreros-Castillo P., Snook L. and Mize C. (2003) Regenerating mahogany (Swietenia macrophylla) from seed in Quintana Roo, Mexico: The effects of sowing method and clearing treatment. *Forest Ecology and Management* **183**, 351-362.

Nooren K., Hoek W., van der Plicht H., Sigl M., van Bergen M., Galop D., Torrescano-Valle N., Islebe G., Huizinga A., Winkels T. and Middelkoop H. (2017) Explosive eruption of El Chichon volcano (Mexico) disrupted 6th century Maya civilization and contributed to global cooling. *Geology* **44**, 175-178.

Patterson R. and Kumar A. (2002) A review of current testate rhizopod (thecamoebian) research in Canada. *Palaeogeography, Palaeoclimatology, Palaeoecology* **180**, 225-251.

Peros M., Collins S., G'Meiner A., Reinhardt E. and Pupo F. (2017) Multistage 8.2kyr event revealed through high-resolution XRF core scanning of Cuban sinkhole sediments. *Geophysical Research Letters* **44**, 7374-7381.

Reimer P. J., Bard M.G.L., Bayliss A., Beck J.W., Blackwell P.G., Ramsey C.B., Buck C.E., Edwards R.L., Freidrich M., Groots P.M., Guilderson T.P., Haflidason H., Hajdas I., Hatté C., Heaton T.J., Hoffmann D.L., Hogg A.G., Hughen K.A.,Kaiser K.F., Kromer B., Manning S.W., Nui M., Reimer R.W., Richards D.A., Scott E.M., Southon J.R., Turney C.S.M., and van der Plicht J. (2013), IntCal13 and Marine13 radiocarbon age calibration curves, 0-50,000 years Cal BP. *Radiocarbon* **55**, 1896-1887. Schmitter-Soto.

Rissolo D., Rodríguez J., and Ball J. (2005). A reassessment of the middle Preclassic in northern Quintana Roo. *Quintana Roo Archaeology*, 66-76.

Sanchez M., Alcocer J., Escobar E., and Lugo A. (2002) Phytoplankton of cenotes and anchialine caves along a distance gradient from the northeastern coast of Quintana Roo, Yucatan Peninsula. *Hydrobiologia* **467**, 79-89.

Schneider T., Bischoff T. and Haug G. (2014) Migrations and dynamics of the intertropical convergence zone. *Nature* **513**, 45-53.

Scott D., and Hermelin J. (1993) A device for precision splitting of micropaleontological samples in liquid suspension. *Journal of Paleontology* **67**, 151-154.

Scott D., Medioli F., and Schafer C. (2001) Monitering in coastal environments using foraminifera and thecamoebians. *Cambridge University Press, New York, USA.*

Smart P.L, Beddows P.A., Doerr S., Smith S.L. and Whitaker F.F. (2006) Cave development on the Caribbean coast of the Yucatan Peninsula, Quintana Roo, Mexico. *Geological Society of America Special Paper 404: Perspectives on Karst Geomorphology, Hydrology, & Geochemistry* **2404**, 105-128.

Stoessel R. (1995) Dampening of transverse dispersion in the halocline in karst limestone in the northeastern Yucatan Peninsula. *Groundwater* **33**, 366-371.

Stoessel R. and Coke J. (2006) An explanation for the lack of dilute freshwater lens in unconfined tropical aquifers: Yucatan example. *Gulf Coast Association of Geological Societies Transactions* **56**, 785-792.

van den Broeke M., Bamber J., Ettema J., Rignot E., Schrama E., van de Berg W.J., van Meijgaard E., Velicogna I. and Wouters B. (2009) Partitioning recent Greenland mass loss. *Science* **326**, 984-986.

van Hengstum P., Reinhardt E., Beddows P., Huang R., and Gabriel J. (2008) Thecamoebians (testate amoeba) and foraminifera from three anchialine cenotes in Mexico: Low salinity (1.5-4.5 psu) faunal transitions. *The Journal of Foraminifera Research* **38**, 305-317.

van Hengstum P., Reinhardt E., Beddows P., Schwarcz H., and Gabriel J. (2009) Foraminifera and testate amoebae (thecamoebians) in an anchialine cave: Surface distributions from Aktun Ha (Carwash) cave system, Mexico. *Limnology and Oceanography* **54**, 391-396.

van Hengstum P., Reinhardt E., Beddows P., and Gabriel J. (2010) Linkages between Holocene paleoclimate and paleohydrology preserved in a Yucatan underwater cave. *Quaternary Science Reviews* **29**, 2788-2798.

van Hengstum P. and Scott D. (2011) Ecology of foraminifera and habitat variability in and underwater cave: distinguishing anchialine versus submarine cave environments. *The Journal of Foraminiferal Research* **41**, 201-229.

Wanner H., Beer J., Bütikofer J., Crowley T., Cubasch U., Flückiger J., Goosse H., Grosjean M., Joos F., Kaplan J., Küttel M., Müller S., Prentice C., Solomina O., Stocker T.,

Tarasov P., Wagner M. and Widmann M. (2008) Mid- to Late Holocene climate change: an overview. *Quaternary Science Reviews* **27**, 1791-1828.

Wanner H., Solomina O., Grosjean M., Ritz S. and Jetal M. (2011) Structure and origin of Holocene cold events. *Quaternary Science Reviews* **30**, 3109-3123.

Ward W. and Brady M. (1979) Strandline sedimentation of carbonate grainstones, Upper Pleistocene, Yucatan Peninsula, Mexico. *American Association of Petroleum Geologists Bulletin* **63**, 362-369.

Ward W., Weidi A. and Back W. (1985) Geology and hydrogeology of the Yucatan and Quaternary geology of Northeastern Yucatan Peninsula. *New Orleans Geological Society*, 1-160.

Ward W. (2004) Geology of coastal islands northeastern Yucatan Peninsula. In V. Leonard and T. Quinn (Eds.), *Geology and Hydrogeology of Carbonate Islands* (275-300), Neatherlands, Amsterdam: Elsevier Science.

3.9 Figures

Fig.1- Map of study area along coast of Yucatan Peninsula, Mexico. Red circles denote study site, Carwash Cenote, as well as other paleoclimate record sites. Grey circles denote locations of current cities.

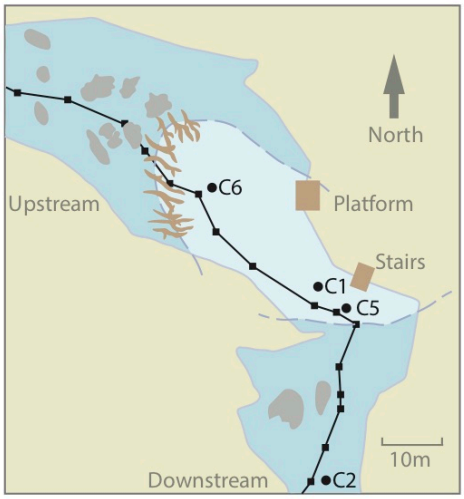

Fig.2- Map of Carwash Cenote. Black circles denote core locations, and black circles along line denote location of cave survey line. Light blue denotes open water cenote, while darker blue denotes cave passage. Karst is denoted by tan, boulders denotes by grey and branches denoted by brown.

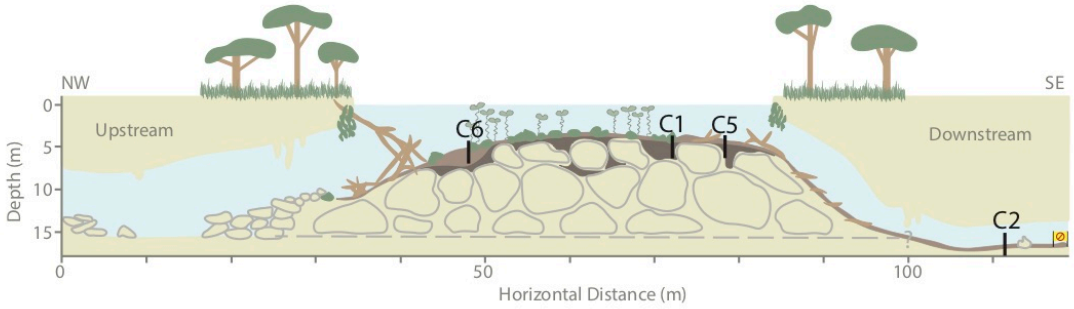

Fig. 3- Depth profile of Carwash Cenote. Core locations are denoted by black lines. Colour denotations from previous figure hold true with dark brown representing peat and lighter brown representing other sediment.

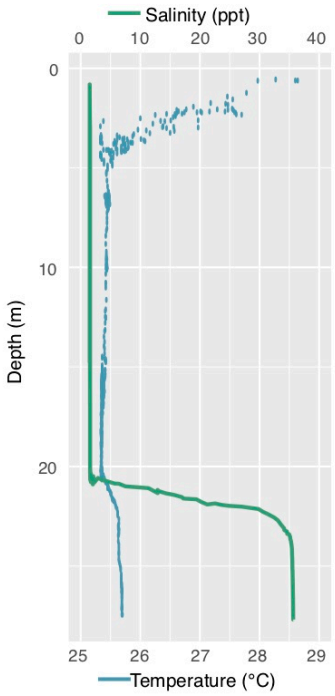

Fig. 4- Salinity and temperature depth profile of Carwash cave system originally published in Kovacs et al. (2017b). Salinity is represented by the solid green line. Temperature is represented by blue dots.

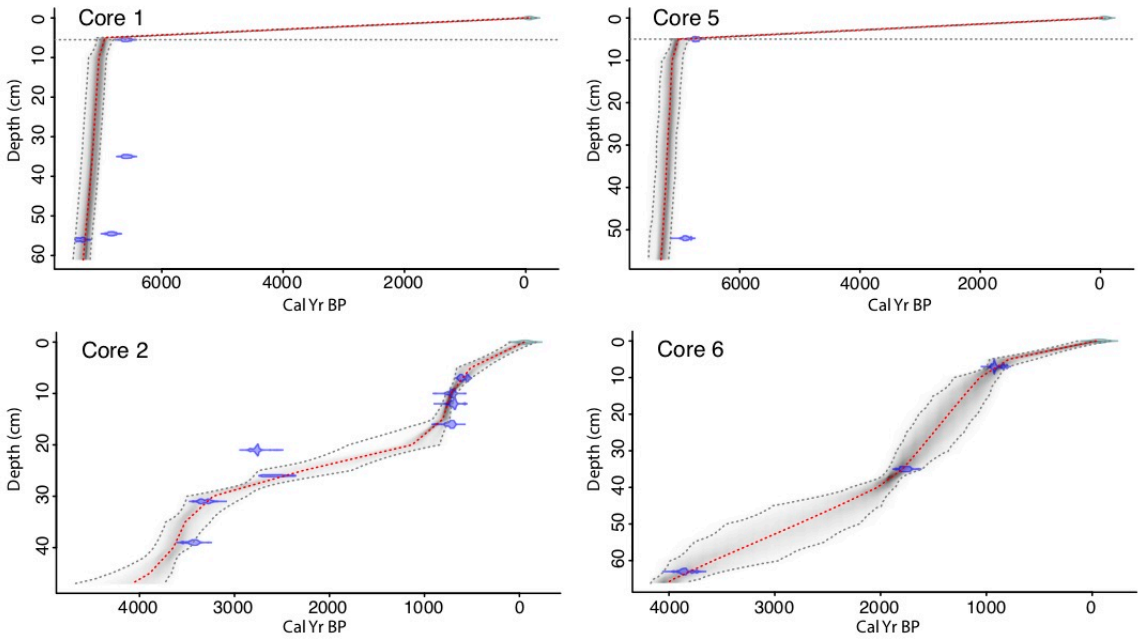

Fig. 5- Age models constructed for cores 1, 2, 5 and 6 using Bacon 2.3 (Balauw and Christen, 2011). Blue dotes represent calibrated distribution of date material. Red dotted line represents calibrated mean and grey area represents calibrated age ranges (yrs. BP) at 2σ confidence intervals.

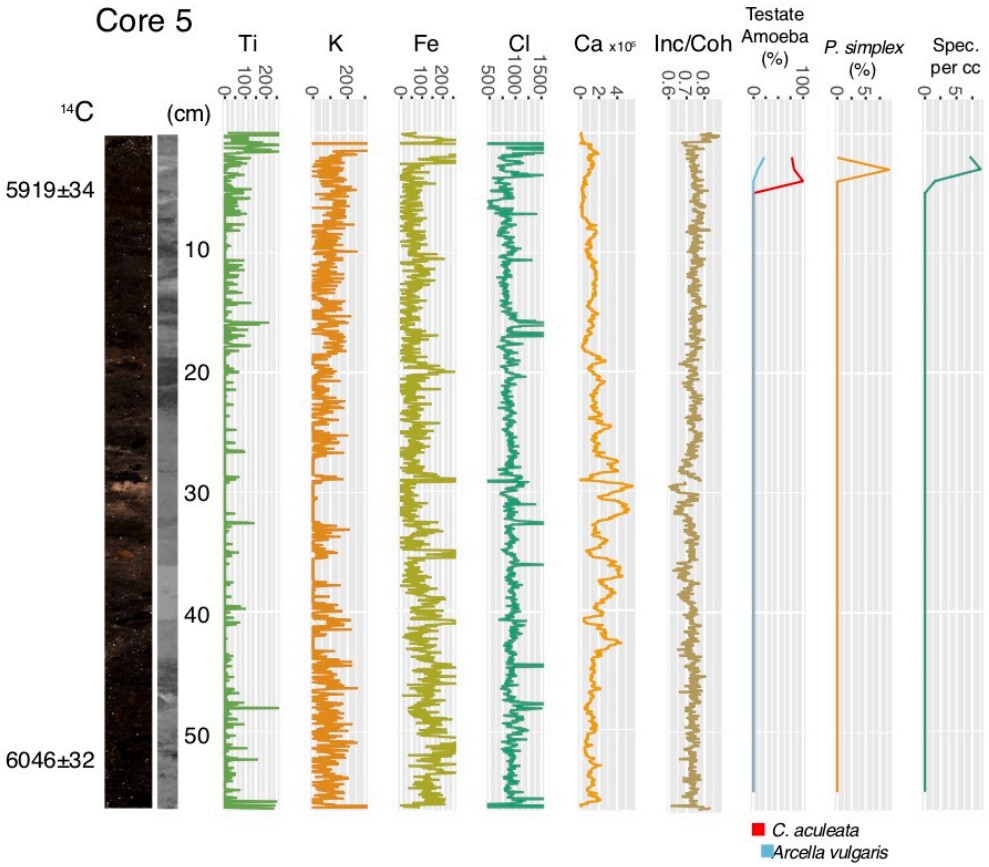

Fig. 6- Core 5 with radiocarbon dates, µXRF (Ti, K, Fe, Ca and Inc/Coh) and microfossil data (testate amoeba and *P. simplex*). Radiocarbon dates are in yrs BP, µXRF in total counts per 500µm and microfossil data in percent of total counted specimens as well as total specimens per cc.

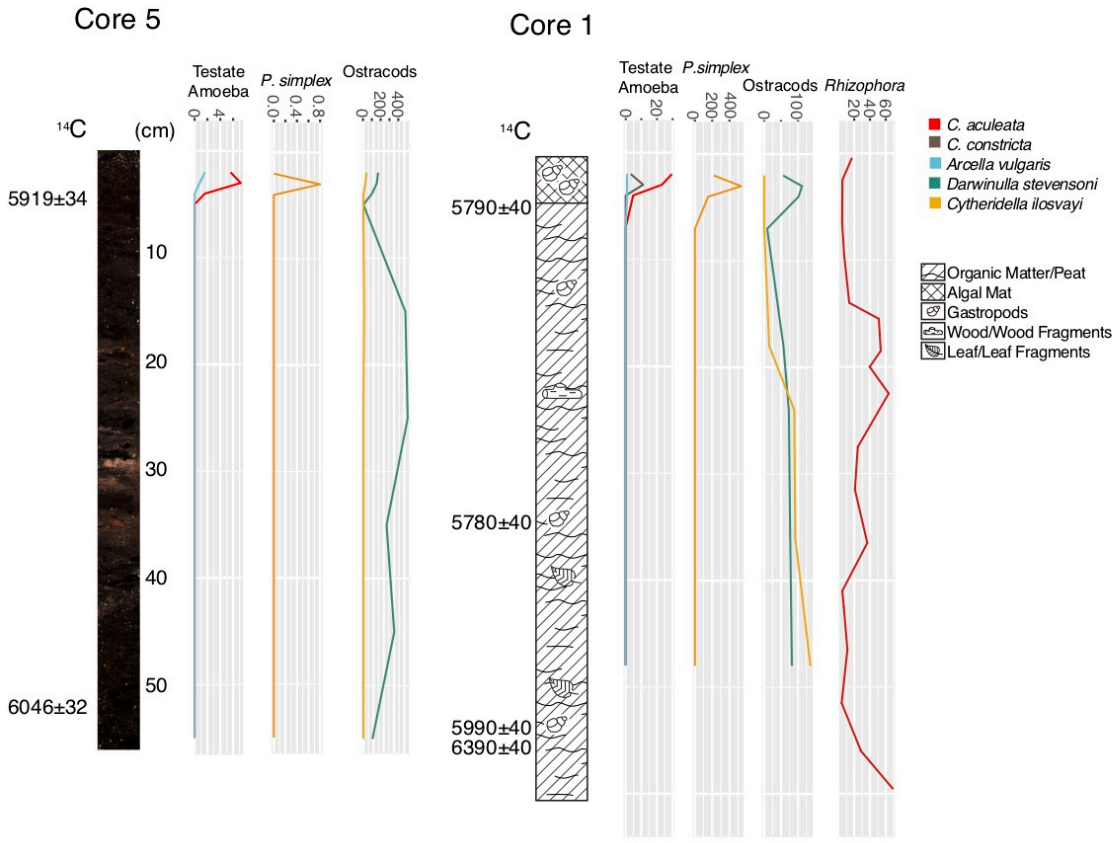

Fig. 7- Comparison of core 5 and 1 with radiocarbon dates, microfossil (testate amoeba and *P. simplex*) and pollen data (*Rhizopora*). Radiocarbon dates are in yrs BP and microfossil and pollen data is in specimens per cc.

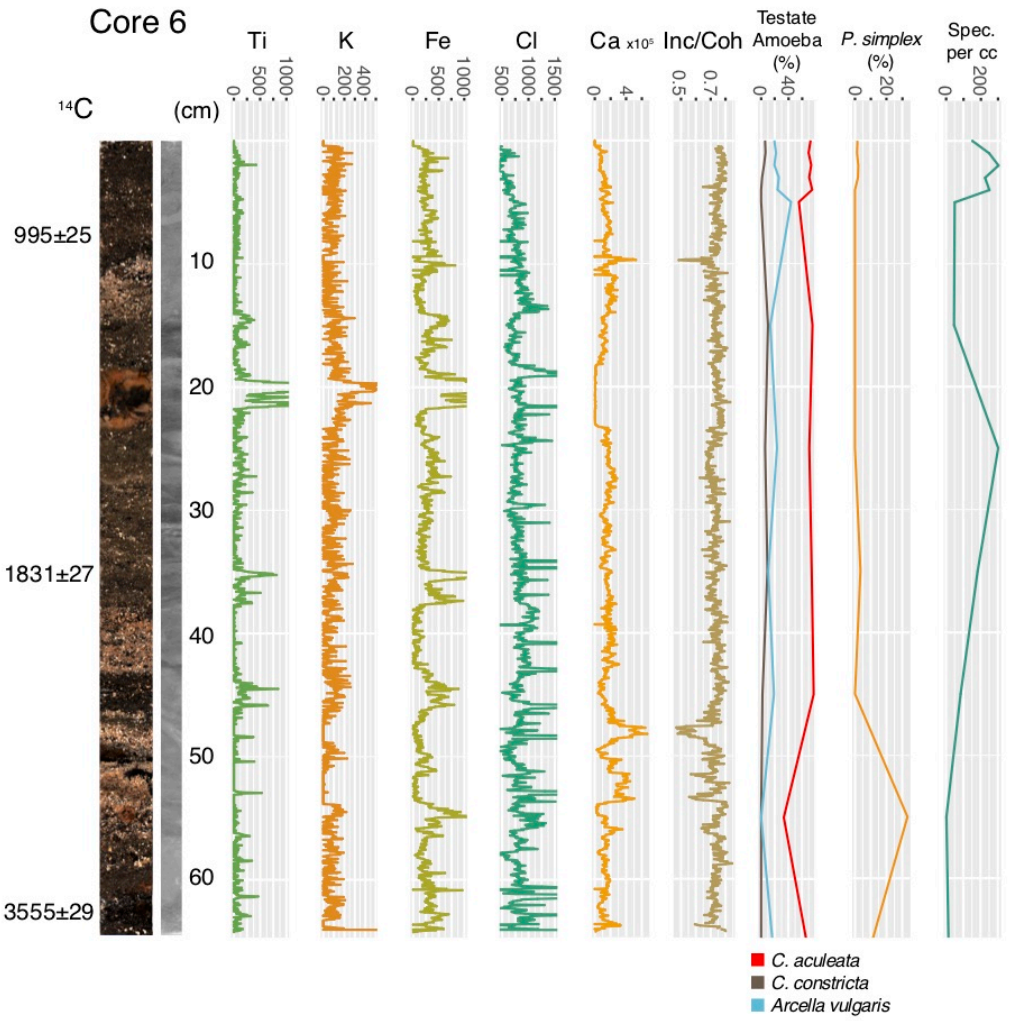

Fig. 8- Core 6 with radiocarbon dates, µXRF (Ti, K, Fe, Ca and Inc/Coh) and microfossil data (testate amoeba and *P. simplex*). Radiocarbon dates are in yrs BP, µXRF in total counts per 500µm and microfossil data in percent of total counted specimens as well as total specimens per cc.

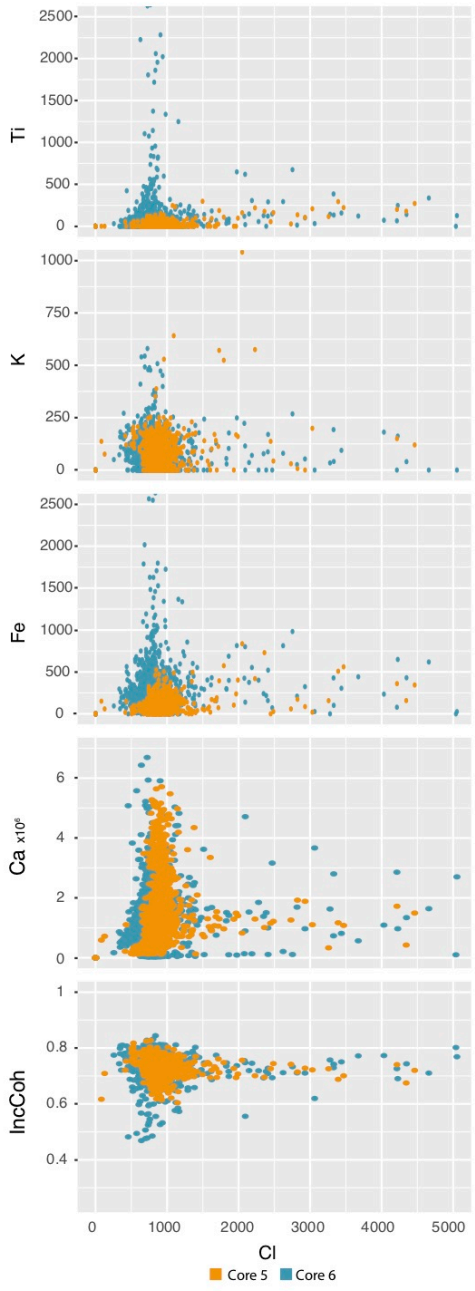

Fig. 9- Cross-plots of core 5 and 6 Cl total counts against Ti, K, Fe, Ca and Inc/Coh total counts. Core 5 values are shown in orange and core 6 values in blue.

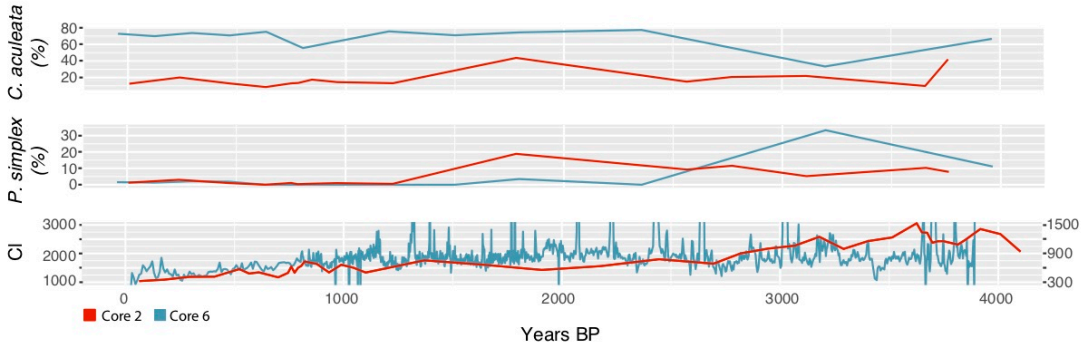

Fig. 10- Comparison of core 2 and 6 µXRF (Cl) and microfossil data (*P. simplex* and *C. aculeata*) against yrs BP. Red lines represent core 2 (with left-side y-axis for Cl graph) and blue lines represent core 6 (with right-side y-axis for Cl graph). Cl is in total counts per 500µm and microfossil data is in percent of total counted specimens.

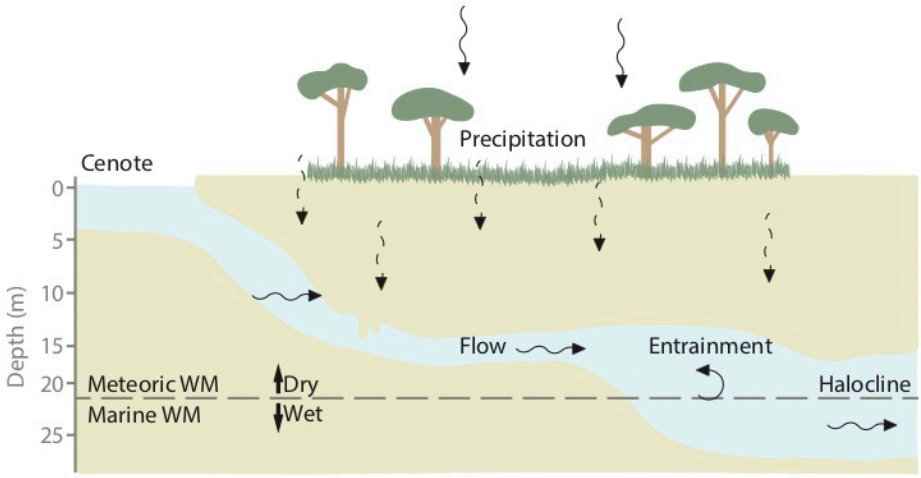

Fig. 11- Conceptual diagram of hydrological processes that affect Yucatan coastal aquifers.

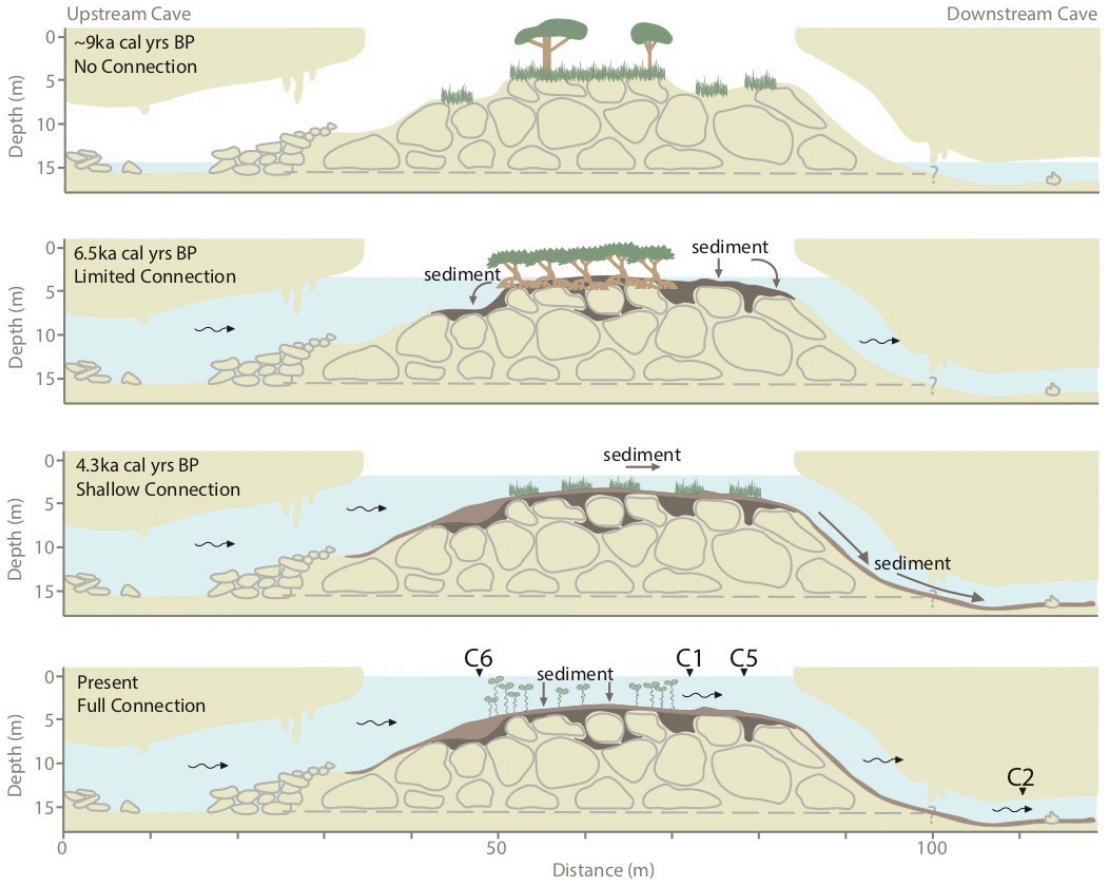

Fig. 12- Flooding history and sediment deposition pattern of Carwash Cenote based off sediment cores and Mexico sea-level curve published by Khan et al (2017).

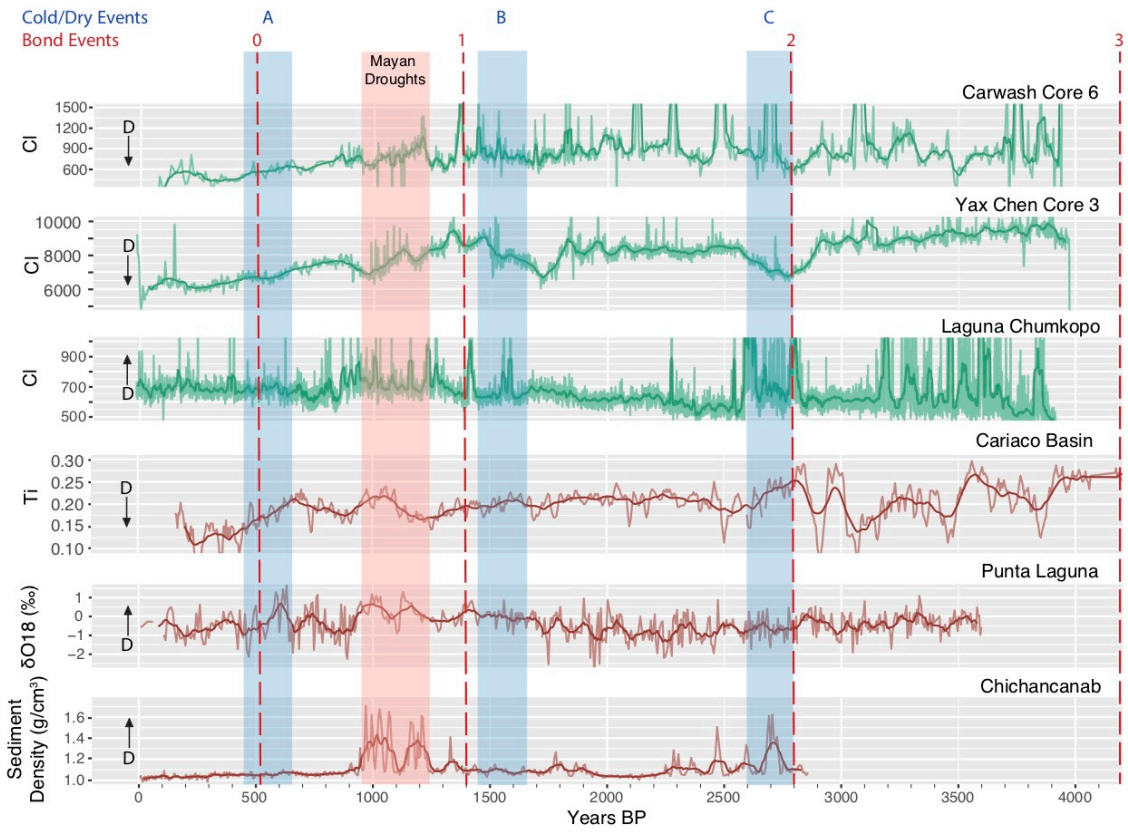

Fig. 13- Carwash core 6 Cl paleoclimate record compared to paleoclimate records from Yax Chen (Cl; Chan et al., 201), Laguna Chumkopop (Cl; McNeill-Jewer et al., in prep.), Cariaco Basin (Ti; Haug et al., 2001), Punta Laguna (δ18O; Curtis et al., 1996) and Lake Chichancanab (sediment density; Hodell et al., 2005). Cl records are represented by green lines and all other records represented by red lines. All records are smoothed by an ~50-100 year running average which is represented by a darker line. Red box represents timing of Maya Terminal Droughts based off both records and previous paleoclimate records. Bond events are represented by dashed red lines and cold/dry events by blue boxes. Cold/dry events are A) Little Ice Age 1300-1500 C.E., B) Dark Age/Migration Period Cooling 300-500 C.E. and C) Late Bronze Age Collapse 2.8-2.6 ka BP (Wanner et al., 2011).

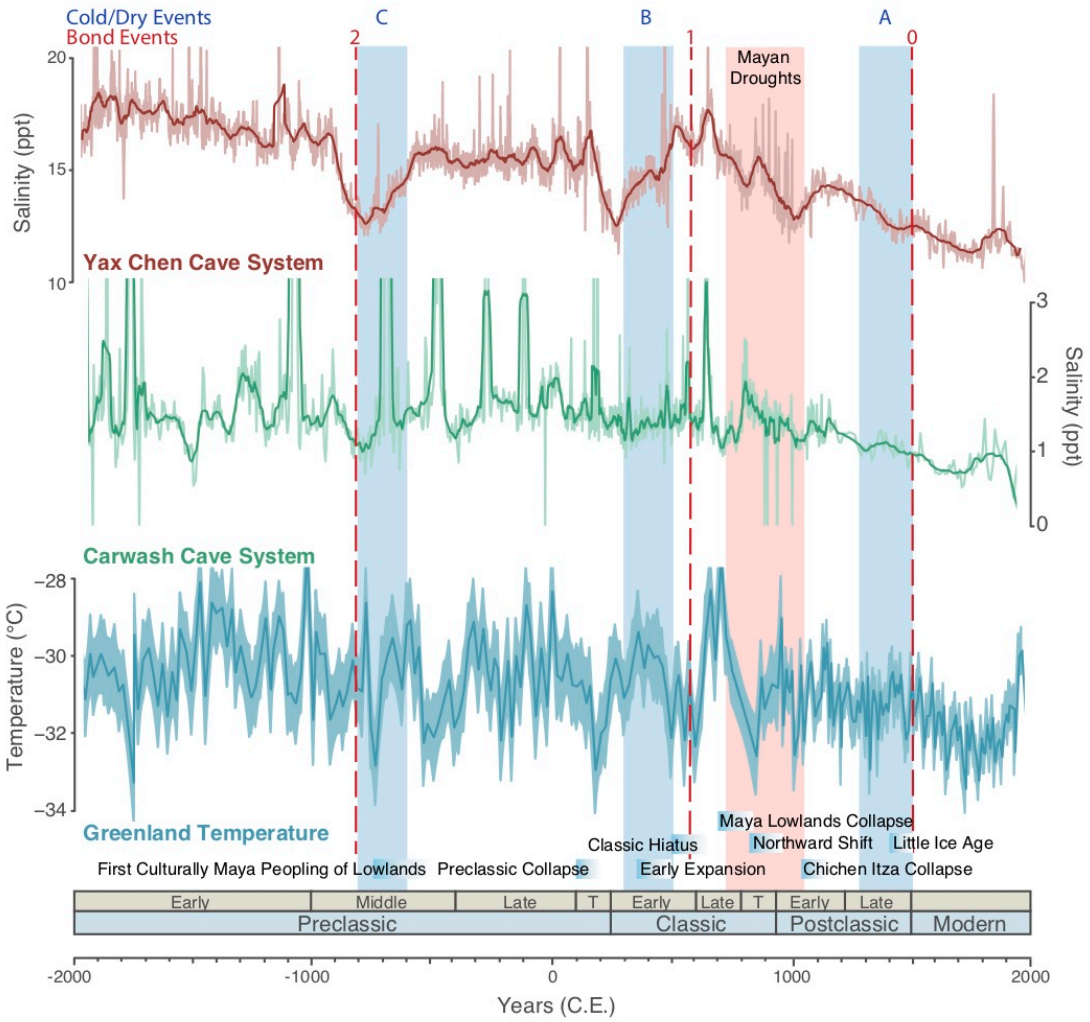

Fig. 14- Salinity records from Carwash core 6 and Yax Chen core 4 and average temperature record from Greenland with major Maya archeological events. The Greenland temperature record comes from the GISP2 ice core from the summit region of central Greenland and temperature was reconstructed by using δ^{15}N and δ^{40}Ar gas fractionation within air bubbles in the ice to measure temperature gradients over time, which were then incorporated into a firn densification/heat diffusion model (Kiboshi et al., 2011). Records have been converted from Cl counts to ppt using equation created by

McNeill-Jewer et al (in prep.). Yax Chen record is represented by red line and Carwash record is represented by green line, both records have a darker line that represents an ~50-100 yr running average. The Greenland temperature record is represented with a dark blue line, lighter blue band representing the 1σ error. Red box represents timing of Maya Terminal Droughts based off both records and previous paleoclimate records. Bond events are represented by dashed red lines and cold/dry events by blue boxes. Cold/dry events are A) Little Ice Age 1300-1500 C.E., B) Dark Age/Migration Period Cooling 300-500 C.E. and C) Late Bronze Age Collapse 2.8-2.6 ka BP (Wanner et al., 2011).

3.10 Tables

Table 1- Radiocarbon results from Carwash Cenote.

Core	Lab ID UOC	(cm)	Material	^{14}C Age (±2σ yr BP)	Cal yr BP (2σ)	C.E./B.C.E.
5	6378	5	Twig	5919±34	6840-7115	5098-4823
	6379	52	Twig	6046±32	7154-7452	5435-5128
6	6380	7	Twig	995±25	782-1002	1015-1235
	6381	35	Twig	1831±27	1601-1930	87-416
	6382	63	Twig	3555±29	3486-4050	2033-1469

CHAPTER 4-CONCLUSIONS

Sediment records within cave systems and lakes in the Yucatan aquifer provide a wealth of information on climate and hydrological changes throughout the Holocene. Previous work has looked at these changes in the short and long term using a variety of proxies. Lakes have typically been seen as closed to the aquifer, therefore investigating connectivity previously has not been investigated which leads to assumptions in regards to paleoclimatic record interpretations. Changes in salinity of the coastal aquifer throughout the Holocene has been focused on in few studies. µXRF data has proved to be a very useful tool when looking at short and long-term changes within water bodies due to its high resolution. This dissertation describes changes through the Holocene to the Yucatan aquifer (both coastal and inland), how sea-level rise has impacted lakes and cave systems and how both local and global climatic changes have influenced hydrology of the aquifer, which may have in turn impacted local populations.

In the first project, sediment cores provided evidence of impact of sea-level rise on lake water level and reduced weathering input during the Terminal Classic. Methodology consisted of microfossil analyses, µXRF data including Ti, K, Fe, Ca and Inc/Coh, radiocarbon dating, water column characteristics and water depth monitoring. Pac Chen Lake water level was found to be largely controlled by Holocene sea-level rise. Short term water level appears to be influenced by tides as it showed a diurnal tidal change. These observations suggest that Pac Chen has been connected to the aquifer to some extent, the magnitude of which has likely been changing over time. Reduced

terrigenous input along the shallow margin indicated reduced rainfall during the Terminal Classic coincided with the timing of the Classic Maya Droughts. However, due to the connectivity of Pac Chen, no water level drawdown was seen. Future studies in the Yucatan should consider the possibility of lake connection to the aquifer as this can affect interpretations due to how changes in the aquifer may impact the water body over time.

In the second project, sediment core records provided evidence of salinity changes within the coastal aquifer throughout the Late Holocene. Methodology consisted of microfossil analyses, µXRF data including Ti, K, Fe, Cl, Ca and Inc/Coh as well as radiocarbon dating. The Carwash cave system was found to evolve through four phases alongside Caribbean sea-level rise. The Cl record from Carwash and Yax Chen revealed an overall freshening of the coastal aquifer through the Late Holocene. Distinct freshening events coincided with global cold/dry events and decreases in Greenland temperature, indicating a hydrological response to global climate cycles. Variations within and between salinity records were determined to be due to proximity to the halocline. The aquifer recorded a drying/freshening trend through the Terminal Classic, coinciding with postulated periods of droughts. Freshening and therefore potability of the coastal aquifer may have led to the survival of coastal Maya communities during this time. Further studies should examine a wider spatial variety of groundwater resources along the Yucatan coast to determine the potability of water sources through the Terminal Classic.

References

Beddows P. (2004) Groundwater hydrology of a coastal conduit carbonate aquifer: Caribbean coast of the Yucatán Peninsula, México (Doctoral dissertation, University of Bristol).

Brenner M., Rosenmeier M., Hodell D. and Curtis J. (2002) Paleolimnology of the Maya Lowlands: Long-term perspectives on interactions among climate, environment, and humans. *Ancient Mesoamerica* **13**, 141-157.

Chan W. M. (2017) Paleohydrologic reconstruction of Yax Chen Cave (Yucatan Peninsula, Mexico) in response to Holocene climate change (Master's Thesis).

Collins S., Reinhardt E., Rissolo D., Chatters J., Nava Blank A. and Luna Erreguerena P. (2015) Reconstructing water level in Hoyo Negro, Quintana Roo, Mexico, implications for early Paleoamerican and faunal access. *Quaternary Science Reviews* **124**, 68-83.

Coutino A., Statsna M., Kovacs S. and Reinhardt E. (2017) Hurricanes Ingrid and Manuel (2013) and their impact on the salinity of the Meteoric Water Mass, Quintana Roo, Mexico. *Journal of Hydrology* **551**, 715-729.

Curtis J., Hodell D. and Brenner M. (1996) Climate variability on the Yucatan Peninsula (Mexico) during the past 3500 years, and implications for Maya cultural evolution. *Journal of Quaterary Research* **46**, 37-47.

Dahlin B. (2002) Climate change and the end of the classic period in Yucatan: Resolving a paradox. *Ancient Mesoamerica* **13**, 327-340.

Douglas P., Pagani M., Canuto M., Brenner M., Hodell D., Eglington T. and Curtis J. (2015) Drought, agricultural adaptation and sociopolitical collapse in the Maya Lowlands. *Proceedings of the National Academy of Sciences* **112**, 5607-5612.

Flores-Nava, A. (1994). Some limnological data from five water bodies of Yucatan as a basis for agriculture development. *Anales del Instituto de Ciencias del Mar y Limnologia* **1-2**, 1-153.

Gabriel J., Reinhardt E., Peros M., Davidson D., van Hengstum P., and Beddows P. (2008) Paleoenvironmental evolution of Cenote Aktun Ha (Carwash) on the Yucatan Peninsula, Mexico and its response to Holocene sea-level rise. *Journal of Paleolimnology* **42**, 199-213.

Gill R., Mayewski P., Nyberg J., Huag G. and Peterson L. (2007) Drought and the Maya collapse. *Ancient Mesoamerica* **18**, 283-302.

Haug G., Gunther D., Peterson L., Sigman D., Hughen K. and Aeschlimman B. (2003) Climate change and the collapse of the Maya civilization. *Science* **299**, 1731-1735.

Hodell D., Brenner M., Curtis J. (2005) Terminal Classic drought in the northern Maya lowlands inferred from multiple sediment cores in Lake Chichancanab (Mexico). *Quaternary Science Reviews* **24**, 1413-1427.

Kennett D., Breitenbach S., Aquino V., Asmerom Y., Awe J., Baldini J., Bartlein P., Culleton B., Ebert C., Jazwa C., Macri M., Marwan N., Polyak V., Prufer K., Ridley H., Sodemann H., Winterhalder B., and Haug G. (2012) Development and disintegration of Maya political systems in response to climate change. *Science* **338**, 788-791.

Kovacs S., Reinhardt E., Chatters J., Rissolo D., Schwarcz H., Collins S., Kim S.T., Nava Blank A. and Luna Erreguerena P. (2017) Calcite raft geochemistry as a hydrological proxy for Holocene aquifer conditions in Hoyo Negro and Ich Balam (Sac Actun Cave System), Quintana Roo, Mexico. *Quaternary Science Reviews* **10**, 205-214.

Kovacs S., Reinhardt E., Statsna M., Coutino A., Werner C., Collins S., Devos F., Le Maillot C. (2017) Hurricane Ingrid and Tropical Storm Hanna's effects on the salinity of the coastal aquifer, Quintana Roo, Mexico. *Journal of Hydrology* **551**, 704-714.

Kovacs S., Reinhardt E., Werner C., Kim S.T., Devos F., and Le Maillot C. (2018) Seasonal trends in calcite-raft precipitation from cenotes Rainbow, Feno and Monkey Dust, Quintana Roo, Mexico: Implications for paleoenvironmental studies. *Palaeogeography, Palaeoclimatology, Palaeoecology* **497**, 157-167.

Masson M. (2012) Maya collapse cycles. *Proceedings of the National Academy of Sciences* **109**, 18237-18238.

McNeil C., Burney D. and Burney L. (2010) Evidence disputing deforestation as the cause for the collapse of the ancient Maya polity of Copan, Honduras. *Proceedings of the National Academy of Sciences of the United States of America* **107**, 1017-1022.

Medina-Elizalde M., Burns S., Lea D., Asmerom Y., Gunten L., Polyak V., Vuille M., and Kalmalker A. (2010) High resolution stalagmite climate record from the Yucatan Peninsula spanning the Maya terminal classic period. *Earth and Planetary Science Letters* **298**, 255-262.

Medina-Elizalde M., Polanco-Martinez J., Lases-Hernandez F., Bradley R. and Burns S. (2016) Testing the "tropical storm" hypothesis of Yucatan Peninsula climate variability during the May Terminal Classic Period. *Quaternary Research* **86**, 111-119.

Nooren K., Hoek W., van der Plicht H., Sigl M., van Bergen M., Galop D., Torrescano-Valle N., Islebe G., Huizinga A., Winkels T. and Middelkoop H. (2017) Explosive eruption of El Chichon volcano (Mexico) disrupted 6th century Maya civilization and contributed to global cooling. *Geology* **44**, 175-178.

Smart P.L, Beddows P.A., Doerr S., Smith S.L. and Whitaker F.F. (2006) Cave development on the Caribbean coast of the Yucatan Peninsula, Quintana Roo, Mexico. *Geological Society of America Special Paper 404: Perspectives on Karst Geomorphology, Hydrology, & Geochemistry* **2404***,* 105-128.

Stoessel R. (1995) Dampening of transverse dispersion in the halocline in karst limestone in the northeastern Yucatan Peninsula. *Groundwater* **33**, 366-371.

Stoessel R. and Coke J. (2006) An explanation for the lack of dilute freshwater lens in unconfined tropical aquifers: Yucatan example. *Gulf Coast Association of Geological Societies Transactions* **56**, 785-792.

Ward W., Weidi A. and Back W. (1985) Geology and hydrogeology of the Yucatan and Quaternary geology of Northeastern Yucatan Peninsula. *New Orleans Geological Society*, 1-160.